

EU PVSEC PAPER

Progress in thin film CIGS photovoltaics – Research and development, manufacturing, and applications

Thomas Feurer^{1*}, Patrick Reinhard², Enrico Avancini¹, Benjamin Bissig¹, Johannes Löckinger¹, Peter Fuchs¹, Romain Carron¹, Thomas Paul Weiss¹, Julian Perrenoud², Stephan Stutterheim², Stephan Buecheler¹ and Ayodhya N. Tiwari¹

¹ Laboratory for Thin Films and Photovoltaics, Empa-Swiss Federal Laboratories for Materials Science and Technology, Ueberlandstrasse 129, 8600 Dübendorf, Switzerland

² Flisom AG, Ueberlandstrasse 129, 8600 Dübendorf, Switzerland

ABSTRACT

This review summarizes the current status of $\text{Cu}(\text{In,Ga})(\text{S,Se})_2$ (CIGS) thin film solar cell technology with a focus on recent advancements and emerging concepts intended for higher efficiency and novel applications. The recent developments and trends of research in laboratories and industrial achievements communicated within the last years are reviewed, and the major developments linked to alkali post deposition treatment and composition grading in CIGS, surface passivation, buffer, and transparent contact layers are emphasized. Encouraging results have been achieved for CIGS-based tandem solar cells and for improvement in low light device performance. Challenges of technology transfer of lab's record high efficiency cells to average industrial production are obvious from the reported efficiency values. One section is dedicated to development and opportunities offered by flexible and lightweight CIGS modules. Copyright © 2016 John Wiley & Sons, Ltd.

KEYWORDS

CIGS; solar cells; review; alkaline; tandem; grading; buffer; passivation

*Correspondence

Thomas Feurer, Laboratory for Thin Films and Photovoltaics, Empa-Swiss Federal Laboratories for Materials Science and Technology, Ueberlandstrasse 129, 8600 Dübendorf, Switzerland.

E-mail: thomas.feurer@empa.ch

Received 25 May 2016; Revised 20 July 2016; Accepted 17 August 2016

1. INTRODUCTION

$\text{Cu}(\text{In,Ga})(\text{S,Se})_2$ (CIGS)-based thin film solar cells represent one of the most promising photovoltaic (PV) technology, with steadily increasing champion cell efficiencies up to 22.6% [1] reported for laboratory scale absorbers. Efficiencies above 20% have been achieved on rigid and flexible substrates by different research institutes as well as industrial companies (see overview in Table I+II). Key advantages of CIGS compared with other conventional PV technologies include the high energy yield (kWh/KWp installed), low temperature coefficient of power loss, low sensitivity to shadowing, and short energy payback time [2–4]. Cost-projections down to 0.35 Euro/Wp have been announced for the current technology, with potential

for further reduction upon scale-up, allowing a significant reduction of the total system cost [5].

The possibility to grow thin films of large area absorber onto a glass as well as lightweight, flexible substrates opens up the field for low-cost manufacturing methods as well as new applications. Applications such as building-integrated PV (BIPV), transport-integrated PV, space flight, or any mobile power generation are market segments where those types of solar modules have greatest advantage compared with traditional PV technologies [46].

In the following, we use CIGS as a general abbreviation for chalcopyrite based solar cells when no specific compositional information is required. The more stringent notation (CIGSe for $\text{Cu}(\text{In,Ga})\text{Se}_2$ or CIGSSe for $\text{Cu}(\text{In,Ga})(\text{S,Se})_2$) is used if differentiation is needed.

Table I. Published efficiencies for a selection of industrial producers. Updated from earlier work [6]. Data for companies not existing anymore are not included. Status: published results until July 2016.

Deposition method	Company	Absorber material	Substrate ^a	Cells intercon. ^b	Reported η [%] (area ^c [cm ²])			Ref. (for η)	Notes
					Cell	Module (M)/	Submodule (S)		
Vacuum-based (direct growth)	Manz - Würth Solar	CIGSe	Glass	Monol.	22.6*	16.0 M		[1, 7]	Collaboration with ZSW
	Solibro (Hanergy)	CIGSe	Glass	Monol.	21.0*			[8, 9]	Record submod.: monol. and grid
	Siva Power	CIGSe	Glass	Monol.	18.8* (0.5)		15.6 (~1 m ²) M, 18.7* (16ap) S	[10]	
	Flisom	CIGSe	PI	Monol.				[11]	Submod. with Empa
	Global Solar Energy (Hanergy)	CIGSe	SS	String	17.7° (1.0ta)	16.9 (10.2da) S		[12]	R2R, Flexible and rigid modules
Vacuum-based precursor	Ascent Solar (TFG Radiant)	CIGSe	PI	Monol.	14*	11.7 M		[13]	–
	Solar Frontier - Showa Shell	CIGSSe	Glass	Monol.	22.8°, 22.3* (0.5da)			[14–16]	Zn(O,S,OH) buffer layer, collab. with NEDO
	Avancis (CNBM)	CIGSSe	Glass	Monol.		17.8 (819ap) S, 17.5* (837.3ap) S, 14.6* (1.228 m ² ta) M		[17]	SiN diffusion barrier
	Miasolé (Hanergy)	CIGSe	SS	Shingle	17	17.9* (622ap)		[18]	R2R, all-sputtering process
	Midsummer	CIGSe	SS	String	17.0 (ap)	16.6° (ap) M 15.5* (1.68m ² ap) M		[19]	Production line for cells (156 × 156 mm), Cd free
	WonCIGS	CIGSSe	Glass	Monol.		16.0* (1.445m ² ta) M, 16.8 (ap) M		[20]	Zn(O,S) buffer, 'turnkey producer'
	NuvoSun (Dow)	CIGSe	SS	String	14 (268)			[21]	Flexible
	HULKet	CIGSe	Glass	Monol.		12.3 (3.555m ² ta) M		[22]	ZnOx buffer
	Stion	CIGSSe	Glass	Monol.	23.2	13.8* (2.348m ² ta)M		[23]	tandem solar cells
						20 (tandem)			

(Continues)

Table I. (Continued)

Deposition method	Company	Absorber material	Substrate ^a	Cells intercon. ^b	Reported η [%] (area ^c [cm ²])			Notes
					Cell	Module (M)/ Submodule (S)	Ref. (for η)	
Non-vacuum-based	Nexcis	CIGS _{Se}	Glass		17.3 (0.5)*			
RTP								
Electrodeposition and precursor selenization	Solopower	CIGSe	SS	Shingle	15.36 (5.4ap)	14.0* (0.7m ² ap) M	[24]	Collab. with IRDEP
						13.4* (3824.6ap) M	[25]	

^aPl, polyimide; SS, stainless steel; \emptyset , no clear information on substrate material.

^bMonol., monolithic;

^cap, aperture area; t, total area; da, designated illumination area.

^dRapid thermal processing.

*Externally certified efficiency.

^ePresented at IW-CIGSTech 7.

1.1. Device structure

Figure 1 shows the typical structure of a CIGS solar cell, indicating some commonly used materials for the different layers. A more detailed description is available elsewhere [47–49]. The most commonly used substrate is rigid, 3–4 mm thick soda-lime glass, as it is thermally stable, chemically inert, and has a similar thermal expansion coefficient as the absorber. It also has a smooth surface, insulating properties suitable for monolithic interconnection and can supply alkali elements for high efficient cells (see section “Alkali post deposition treatment of CIGS layer”). However a significant amount of work has also been performed for CIGS on flexible substrates such as metal foils, ceramics, and polymer films, as discussed in more detail elsewhere [47].

The preferred back contact consists of sputtered molybdenum, serving as a quasi-ohmic contact with the absorber by formation of a MoSe₂ intermediate layer during absorber growth. The *p*-type CIGS absorber can be grown by co-evaporation processes, with selenization followed by sulfurization of precursors deposited by sputtering, electrodeposition, or printing. While co-evaporation led to the highest efficiencies for a long time [32,50,51], the largest commercial manufacturer Solar Frontier is using a sputtered precursor with subsequent selenization and sulfurization and reported a record efficiency of 22.3% [14,15]. Table I and II gives a selected overview of the growth method and efficiencies achieved in different research institutes and companies. Various CIGS compositions are used, mainly aiming at tuning the material band gap (In-Ga ratio, Se-S ratio), as well as its bulk and surface electronic properties. Among others, the introduction of a band gap grading and the presence of alkali elements are two key features that have fueled the development of higher efficiencies in recent years and are addressed in more detail in the following sections.

Following the absorber deposition, heterojunction formation is ensured by the deposition of a thin *n*-type buffer layer. Historically, cadmium sulfide (CdS) has been used for best efficiency, but because of its relatively low band gap (2.4 eV), the search for alternative materials yielding similar junction quality has been given much attention and is discussed further in the sections (see section “Buffer layers”).

Transparent conducting oxides (TCO) are applied as the front contact. Research cells and even some commercial module designs support the charge collection with an additional metallic grid. A typical TCO stack consists of a thin layer of intrinsic zinc oxide followed by aluminum-doped zinc oxide [52]. The intrinsic layer helps in preventing current leakage in case of local inhomogeneities or incomplete buffer coverage [53,54] and also possibly to protect the buffer from ion damage during TCO sputtering.

For record efficiency cells and modules, an anti-reflecting coating is often applied.

Table II. State-of-the-art efficiencies on cell and sub-module level in selected research laboratories. Status: published results until July 2016.

Institute	Country	Cell η [%]	Ref. cell η	Sub-module η [%] (area ^a [cm ²])	Cells intercon. ^b	Ref. sub-mod. η	CIGS deposition method	Substrate ^c	Notes
Solar Frontier	Japan	22.8°, 22.3*	[15]	17.8 (819ap)	monol.	[14]	Sputtering, selenization, and sulfurization (CIGSSe)	Glass	With NEDO and AIST
ZSW	Germany	22.6*	[1]	16.8* (61ap)	monol.	[26]	Co-evaporation (CIGSe)	Glass	–
		21.0*	[27]	15.2 (63ap)	monol.	[28]	Co-evaporation (CIGSe)	Glass	Zn(O,S) buffer layer
NREL	USA	20.8	[29]	–	–	–	Co-evaporation (CIGSe)	Glass	–
		18.6	[30]	–	–	–	Evaporation and selenization	Glass	Zn(O,S) buffer layer
Toshiba Empa	Japan	20.7	[31]	–	–	–	Co-evaporation (CIGSe)	Glass	–
	CH	20.4*	[32]	16.6* (13ap)	monol.	[33]	Co-evaporation (CIGSe)	PI	Flexible polyimide, module with Flisom
AIST	Japan	19.9	[34]	15.9* (69.6 da)	monol.	[35]	Co-evaporation (CIGSe)	Glass/SS	Monol. Interconn. on metal foil
IEC Delaware	USA	19.9	[36]	–	–	–	Co-evaporation (AgCIGSe)	PI	Wide band gap (Ag,Cu)(In,Ga)Se ₂
AGU	Japan	19.7*	[37]	17.8 (819ap)	monol.	[16]	Sputtering, selenization, and sulfurization (CIGSSe)	Glass	Zn(O,S) buffer layer, with Solar Frontier
		18.4	[38]	–	–	–	Co-evaporation (CIGSe)	Glass	Zn(O,S) buffer layer
HZB	Germany	19.4*	[39]	–	–	–	Co-evaporation (CIGSe)	Glass	High growth temperature (>600 °C)
		16.1*	[40]	13.0 (30x30)	monol.	[40]	Sputtering, selenization, and sulfurization (CIGSSe)	Glass	Zn(O,S) buffer layer, with Bosch
Uppsala	Sweden	18.6	[41]	17.4* (16ap)	monol.	[42]	Co-evaporation (CIGSe)	Glass	In-line, module with Solibro
Korea University	Korea	–	–	17.9 (900)	monol.	[43]	Sputtering, selenization, and sulfurization (CIGSSe)	Glass	Zn(O,S) Buffer, with Samsung SDU
IRDEP	France	17.3*	[24]	14.0* (6610ap)	monol.	[24]	Electrodeposition and selenisation (CIGSSe)	Glass	Solution-based precursor, with Nexcis
NREL	USA	11.7*	[44]	–	–	–	Electrodeposition and selenization (CIGSe)	Glass	Solution-based precursor
IBM	USA	15.2*	[45]	–	–	–	Hydrazine-based (CIGSSe)	Glass	Pure solution

^aap, aperture area; t, total area; da, designated illumination area.^bMonol., monolithic.^cPI, polyimide; SS, stainless steel.

*Externally certified efficiency.

°Presented at IW-CIGSTech 7.

2. SOME RECENT ADVANCEMENTS

2.1. Alkali post deposition treatment of CIGS layer

Addition of alkali elements, especially Na, has long been subject of studies in the chalcopyrite thin film community, because of the beneficial impact on the electronic

properties of the absorber and solar cells. If not diffusing directly from the glass substrate during the absorber deposition at elevated temperature [55], similar beneficial effect on the bulk electronic properties were observed when adding them in a controlled manner prior, during, or after CIGS growth [56]. Whereas Na long showed the most beneficial effect, the controlled addition of KF in a post-deposition treatment (PDT) yielded a significant

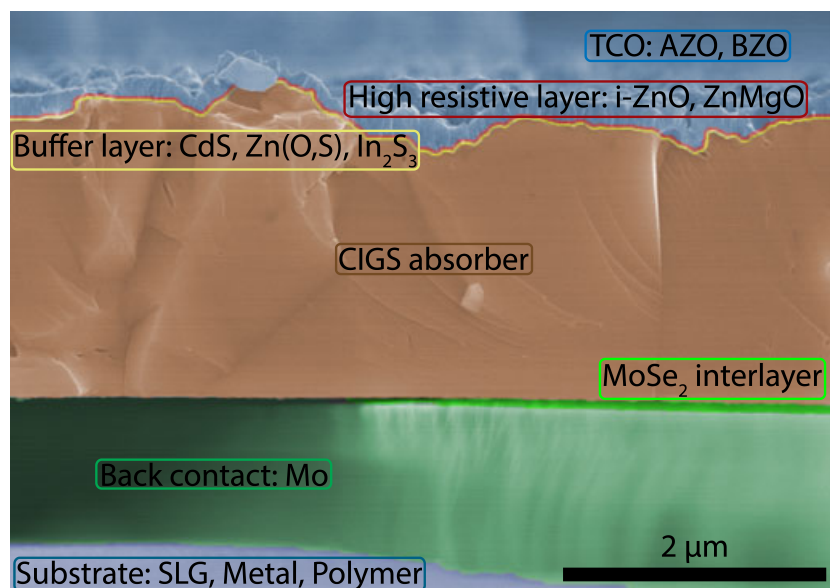


Figure 1. Basic structure of a typical CIGS solar cell, with examples of the most commonly used materials.

improvement in efficiency up to a world record efficiency of 20.4% [32]. Such a PDT treatment was originally found to be the most beneficial method to add Na onto CIGS grown at low-temperature on plastic substrate [57], because it allows separating the influence of Na on CIGS film growth from its beneficial effect on electronic properties. While it was found that Na PDT mainly modifies the bulk electronic properties of the CIGS layer, with no discernible surface modification, addition of KF in a similar PDT treatment leads to a significant alteration of the CIGS surface composition, namely Cu and Ga depletion. Furthermore, a decrease in Na content for samples treated with K is also systematically observed [30,32,58,59], possibly based on an ion exchange mechanism. The modified CIGS surface has strong implications on the interface formation and growth of subsequent layers, especially when grown by chemical bath methods [32,60]. A review of the impact of addition of KF after the growth of CIGS is presented in ref. [11]. Strengthened by several consecutive world records for the CIGS technology when applying a process based on alkali-addition after CIGS growth [51,61,62], this findings shed new light on the importance of considering the alkali addition process together with alkali type and their combination and the effects on both bulks as well as surface/interface properties of CIGS and solar cells. Whether the effect of KF PDT is a direct electronic effect because of the modified surface composition of the CIGS layer or whether it indirectly affects the junction quality by modifying the interface properties during buffer layer deposition is still under discussion. Influence on the bulk properties have also to be considered and cannot be excluded from the overall effects on solar cell efficiency.

In addition to the 1-dimensional vision of the buffer layer-absorber formation, the formation of point contacts

induced by a nano-structuring of the interface could shift the transport characteristics of the carriers from a 1-dimensional to a 2-dimensional model [63]. Overall, the fact that the KF PDT is not only beneficial for co-evaporated absorbers, but also for sputtered and selenized films [30], and even for absorbers with higher Ga content [61], hints that it is likely mostly an interface-related improvement. Latest results using the heavier alkali elements rubidium and caesium have shown an even stronger improvement of properties, leading to the highest certified efficiency to date (22.6%) for a cell with RbF PDT [1]. On the other hand, Solar Frontier has recently announced measurements with an uncertified efficiency of 22.8% for cells with KF PDT at IW-CIGSTech 7. Further research in this direction, based on processes derived from PDT or new knowledge gained during investigation of its mechanism, will likely lead to new record efficiencies.

2.2. Compositional grading in the absorber layer

State-of-the-art CIGS thin film absorbers grown by co-evaporation generally show a varying indium to gallium ratio across their thickness. The relative amount of Ga determines the bandgap energy of CIGS, which can range from 1.0 eV for pure CuInSe₂ to 1.7 eV for pure CuGaSe₂, mainly due to a shift in the position of the conduction band maximum [64]. Average bandgap energy values of 1.1–1.2 eV, corresponding to a [Ga]/([Ga]+[In]) ration of around 0.3 are used in record efficiency devices.

A Ga-grading profile was first introduced by Contreras *et al.* [65] and later extended as a consequence of the introduction of a three-stage deposition

process by co-evaporation [66]. This process, which yields better crystallinity of the absorber layer, is based on the interdiffusion of the different elements and naturally results in the formation of a double grading profile with a higher Ga contents towards the front and the back interfaces, and lower Ga contents in the central-front region. This can be explained by a more favorable reaction between Cu and In than between Cu and Ga [67] and by different potential barriers for the diffusion of In and Ga through Cu vacancy defects [68]. As a consequence, there is a strong interplay between the amount of excess Cu supplied during the 3-stage process, the final overall amount of Cu, and the shape of Ga-grading profile [69,70]. Szaniawski *et al.* [71] reported that interpreting the effects of variations in the Cu content is complicated by the resulting variations in the Ga grading, which could explain the scarcity of studies on the effects of the Cu content in Ga-graded CIGS absorbers. The formation of the Ga grading can also be influenced by other factors such as the presence and amount of alkalis during growth [72–74] and the deposition temperature [75]. The Ga grading resulting from a 3-stage process is typically further controlled by adjusting the In and Ga rates during CIGS growth [69,76].

One of the advantages of a Ga grading in CIGS absorbers is the presence of a back-surface field, which assists the drift of free electrons towards the front junction. This results in an improved collection of charge carriers, especially for photon energies in the near infrared [77]. Another advantage consists in the presence of a low-bandgap ('notch') region close to the front surface, enhancing the absorption of low-energy photons. Larger Ga content at the front interface of the absorber than in the notch ('front grading') is needed for improved junction quality. A small conduction band offset (<0.3 eV) at the CdS/CIGS junction is reportedly beneficial for the interface quality, although a larger offset would result in a potential barrier for electrons and lead to increased interface recombination [78–80].

The ideal shape of the front and back gradings was investigated in depth by computer simulations, however without consensus being reached [68,81,82]. Experimental results reported in 2011 showed that an overly pronounced front grading can also result in a barrier for electrons, leading to enhanced recombination in the space-charged region [76]. To achieve a smoother front grading, the standard 3-stage process was modified into a multi-stage process, with the addition of several sub-stages in the evaporation rates of In and Ga [76]. Jackson *et al.* [51] reported, on the other hand, that an efficiency increase from 20.8% to 21.7% was partially achieved also thanks to a more pronounced front grading. This is however no contradiction, because the optimized Ga-grading profiles reported in Refs. [32] and [51] are similar in the front region of the absorber, as shown in Figure 2.

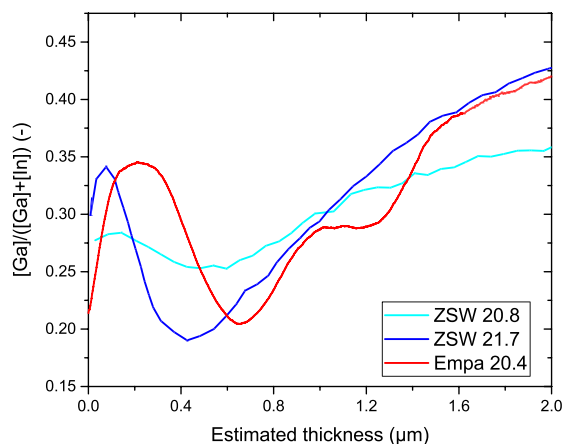


Figure 2. Comparison of published $[Ga]/([Ga] + [In])$ gradings in CIGS solar cells with efficiency $>20\%$ [32,51].

The technical complexity of a 3-stage process motivates investigations for simpler deposition methods. Salome [83] demonstrated in 2014 that, provided the implementation of a workable Ga-grading, a comparable absorber quality can be achieved on single-stage absorbers. The authors reported a small drop in efficiency from 17% of a 3-stage reference to 16.3% of the single-stage, which they attributed mainly to differences in the front surface grading. Mainz *et al.* [84] recently showed that recrystallization of the chalcopyrite phase during co-evaporation of CIS films might occur shortly before the segregation of Cu-Se on the surface. High-quality Cu-poor films could therefore be achieved without reaching a Cu-rich phase at all, which might open up the possibility of a passage to a much simpler and controllable process if the composition and crystal structure during the co-evaporation process is carefully *in situ* monitored. However, the study was performed on Ga-free absorbers and the eventual effect on the Ga grading is therefore unknown.

CIGS layers grown by a two-step process of selenization of a precursor have generally Ga accumulation at the back, near the Mo interface. Such a composition with a Ga depleted front surface is undesirable for high efficiency cells. Therefore precursor and selenization conditions are optimized for appropriately homogenized Ga concentration profile in two-step processed absorbers. However, for the highest efficiency solar cells an additional step of H_2S annealing is used to form a selenium rich $CIGS_{Se}$ layer in order to reach high V_{OC} values [85–87]. $CuInS_2$ and $CuGaS_2$ have a bandgap of 1.53 and 2.49 eV, respectively, extending the systems range considerably. Contrary to Ga, the sulfur incorporation is mainly acting on the valence band minimum [88]. Cells using partial sulfurization reach very high efficiencies, as for example, the current efficiency record of Solar Frontier which most probably involves a sulfurization step. However full-sulfur CIGS (without any selenium) is still limited and reached 15.5% just recently [89].

Table III. Summary of best performing small-area CIGS cells with different buffer layers and respective deposition methods.

Buffer layer	Dep. method	Absorber	Window layer	Eff. (%)	V_{OC} (V)	J_{SC} (mA cm ⁻²)	FF (%)	Area (cm ²)	Ref
CdS	CBD	CIGSe	i-ZnO/ZnO:Al	21.7*	0.746	36.6	79.3	0.5	[51]
Zn(O,S)	CBD	CIGSe	Zn _{0.75} Mg _{0.25} O/ ZnO:Al	21.0*	0.717	37.2	78.6	0.5	[27]
Zn(O,S)	CBD	CIGSSe	ZnO:B	17.9*	0.66 (cell calc.)	38.1	71.1	900	[43]
Zn(O,S)	ALD	CIGSe	ZnO:B	19.8*	0.715	36.5	75.8	0.522	[107]
Zn(O,S)	Sputtering	CIGSe	ZnO:Al	18.3*	0.654	38.4	72.8	0.49	[104]
Zn _{1-x} Mg _x O	ALD	CIGS	i-ZnO/ In ₂ O ₃ :Sn	15.5*	0.92	23.4	72.2	0.433	[89]
Zn _{1-x} Mg _x O	ALD	CIGSe	i-ZnO/ZnO:Al	18.1	0.668	35.7	75.7	0.5	[105]
In _x S _y	Thermal evaporation	CIGSe	i-ZnO/ZnO:Al	18.2	0.673	36.3	74.5	0.5	[106]
Zn _{1-x} Sn _x O _y	ALD	CIGSe	i-ZnO/ZnO:Al	18.2*	0.689	35.1	75.3	0.49	[41]

*Externally certified efficiency.

2.3. Buffer layers

The following section focuses on the most recent advancements in buffer layers in CIGS solar cells since the review by Witte *et al.* [90]. For more details on the development and applications of buffer layers and transparent conducting oxides in CIGS cells, the reader is referred to the extensive reviews by Naghavi *et al.* [54] and Hariskos *et al.* [91].

The highest conversion efficiencies in CIGS solar cells have been commonly achieved using chemical bath deposited (CBD) CdS as a buffer layer [49]. CdS seems to satisfy most requirements of a buffer layer with a suitable conduction band alignment to the absorber and the undoped ZnO and with a beneficial interface defect chemistry. It has been reported that positively charged Cd may form a stable donor-type defect in copper-deficient chalcopyrite surfaces resulting in an appropriate charge density and well defined Fermi-level position [92]. The major disadvantage of CdS is its relatively narrow band gap of about 2.4 eV leading to parasitic absorption losses to the cell current. Hence, an extensive research on alternative buffer layers is ongoing, with Zn(S,O,OH), Zn_{1-x}Mg_xO, In₂S₃, and Zn_{1-x}Sn_xO being the most promising materials to replace CdS so far. Solar Frontier has carried out a pioneering development in the application of CBD grown Zn(S,O,OH) buffer layers, and they use this process in their commercial production. Table III summarizes the champion devices based on the aforementioned buffer layers with their respective deposition methods, and Figure 3 highlights the current gains shown for some of those devices. The best conversion efficiency to date with a confirmed alternative buffer layer (Zn(S,O,OH)) is 21.0% [27] and was made possible by the combination with a new alkali PDT as discussed previously, combined with a Zn_{0.75}Mg_{0.25}O/ZnO:Al window layer deposited by sputtering. The band gap of ZnO_{1-x}S_x is tunable by varying the S/O ratio in between 3.2

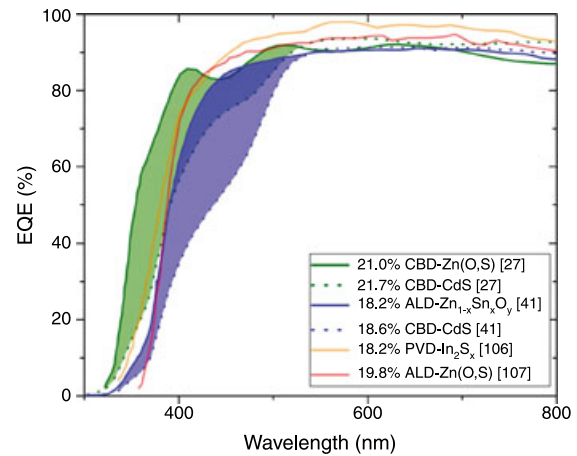


Figure 3. External quantum efficiency for CIGS cells with different buffer materials. All cells with anti-reflection coatings. The shaded areas below the curves represent the current gain relative to the corresponding CdS reference when available. Data extracted from [27,41,106,107].

(E_g, ZnO) and 3.6 eV (E_g, ZnS) with a bowing minimum close to 2.6 eV for $x=0.45$ as reported by different groups [93–95]. Extensive optimization is often needed for an optimal band alignment to avoid metastabilities in the current-voltage measurements, requiring post-deposition treatments such as annealing and/or light soaking [96–98]. In the case of CBD, the similar solubility and complex formation constants of ZnS, Zn(OH)₂, and ZnO, which were investigated, that is, by Hubert *et al.* [99], lead to a co-precipitation demanding for precise control of the deposition conditions. But even for atomic layer deposited Zn(O,S), which is supposed to give the highest control over stoichiometry due to its layer-by-layer growth mode, post-deposition heat-light soaking effects have been reported [100]. The CBD method which currently leads to the highest power

conversion efficiencies in CIGS/Zn(O,S) devices is based on 'Zn²⁺' and 'S²⁻' sources in a NH₃/H₂O medium at elevated temperatures. Current developments focus on faster reaction kinetics, that is, deposition speed, by either exchanging the slowly de-composing thiourea, the established 'S²⁻'-source [101,102], or by the addition of additives [103] to satisfy the needs for an industrial application. For an all-vacuum process, sputter deposited Zn(O,S) achieved an efficiency of 18.3% [104]. Similar efficiencies have been reached with Zn_{1-x}Mg_xO (18.1% [105]) and Zn_{1-x}Sn_xO_y (18.2% [41]) buffer layers deposited by atomic layer deposited. Indium sulfide is also among the most promising alternatives for CdS replacement. Using thermal evaporation, an efficiency of 18.2% [106] has been achieved.

On sub-module scale an efficiency of 17.9% has been achieved recently on 30x30 cm², employing CBD-Zn(S, O,OH) [43]. The same sub-module efficiency was reached using an Indium sulfide [17] buffer layer.

2.4. Surface passivation

Charge carrier recombination at interfaces is still limiting the potential of CIGS solar cells. Concepts for surface passivation attempt to reduce recombination of diode and photocurrent at the absorber front and back interfaces. While the buffer already partly serves this function at the front, in this section, we review the implementation of additional concepts such as structured and insulating passivation layers.

At the back contact interface of the CIGS solar cells, beside the back-surface field induced by the bandgap grading [108], passivation methods based on local point contacts were recently proposed [109], similar to those applied for high efficiency Si-based solar cells [110]. They could lead to improved cell properties especially for very thin or non-graded absorbers, where the grading alone is insufficient to prevent minority carrier recombination at the back contact. Alumina is one of the materials suggested for such applications. It reduces non-radiative recombination as a higher photoluminescence yield was observed for CIGS absorbers passivated with atomic layer deposited Al₂O₃ [111,112]. Kotipalli *et al.* [113] found by capacitance - voltage (CV) measurements either positive or negative surface charge in or at the oxide/CIGS interface dependent on post deposition annealing conditions. Solar Cell Capacitance Simulator (SCAPS) [114] simulations by Vermang *et al.* [109] showed that the surface recombination velocity can be reduced from 10⁴–10⁶ cm s⁻¹ to 10²–10³ cm s⁻¹ for a CIGS device with local point contacts through an Al₂O₃ passivation layer at the back contact. In an experimental implementation of the idea, openings for local rear point contacts were achieved via e-beam lithography [115] or CdS particles [109]. A significant efficiency improvement for thin (<1.6 μm) ungraded absorbers has been observed. However, a beneficial effect of this back contact passivation approach for devices with a Ga grading towards the back contact has not been shown so far. Another effect of

the structured or passivated back contacts is the possibility for better light management. Improvements in the efficiency for thin absorbers have recently been shown by different groups [116,117].

Front contact passivation can be approached in a similar manner to point contacts at the back. Simulations show possible performance improvements by choosing a suitable passivating material with appropriate point opening geometry [63,118–120]. Optimal point contact width and pitch were estimated to be in the 10 nm and 100 nm range respectively, based on current CIGS layer quality. Furthermore, for a good front contact passivation layer, donor-like defects close to the conduction band maximum of the CIGS (positive fixed charge) are preferred to increase the absorber surface inversion [120]. Hultqvist *et al.* [121] have shown that ZnS can act as an effective passivation layer based on CV and photoluminescence measurements on metal-insulator-semiconductor type structures. Indeed, Allsop *et al.* [122] demonstrated experimentally that a thin layer of ZnS between the In₂S₃ buffer and CIGS absorber improves the solar cell performance. Subsequently, Fu *et al.* [123,124] have demonstrated a solar cell with point contacts to the buffer layer and a ZnS passivation layer from ZnS nanodots deposited by a spray-ILGAR method and Reinhard *et al.* [63] demonstrated the self-assembly of nano scale fluoride crystals on the absorber surface, which could serve as a template for passivation layer deposition.

2.5. Transparent contacts and stability behavior

Aluminum doped ZnO (AZO) is the most commonly applied transparent contact on CIGS and is mostly deposited by sputtering. Given the relatively low mobility (<30 cm² V⁻¹ s⁻¹), AZO is heavily doped to achieve the necessary conductivity, leading to optical losses in the visible and near-infrared by free carrier absorption. This is especially problematic when using thick TCOs as required on a module level. Several alternative TCOs have been investigated to reduce free carrier absorption. An alternative, used by Solar Frontier, is chemical vapor deposited boron doped zinc oxide (BZO). High mobilities up to 40 cm² V⁻¹ s⁻¹ have been achieved with CIGS compatible deposition processes, while the carrier density is kept below ~1*10²⁰ cm⁻³ and therefore the TCO transparency and the short circuit current output is increased (Figure 4, left) [125]. Other recent works on high mobility TCOs for CIGS investigate nominally undoped ZnO, hydrogenated indium oxide (IOH) and indium zinc oxide (IZO) [126–129].

Investigations on the long-term stability of CIGS modules have shown that the TCOs are strongly susceptible to degradation in humid atmosphere [133–137]. The conductivity of AZO degrades in humid atmosphere, which is caused by the chemisorption of environmental oxygen species, leading to zinc hydroxide and carbonate formation [138]. Chemisorption leads to the formation of potential barriers at grain boundaries, significantly

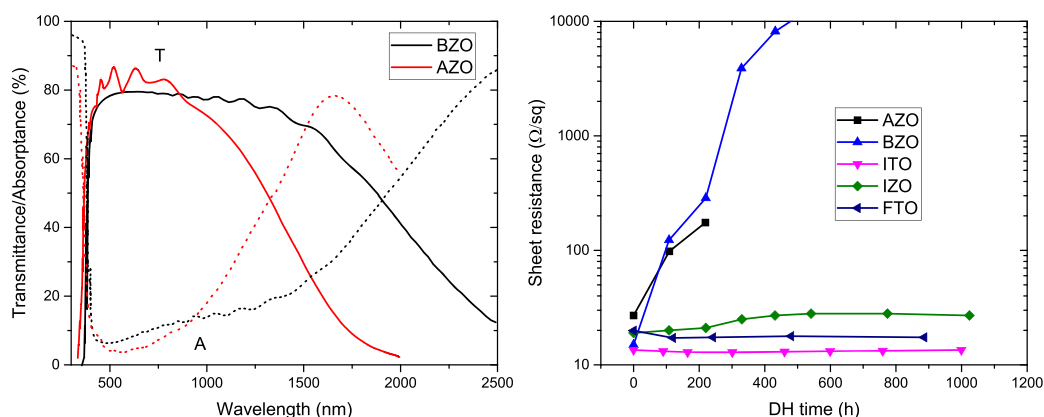


Figure 4. Left: Comparison of the optical properties of AZO and BZO with comparable sheet resistance. The high transmission in the near-infrared region for BZO stems from the reduced carrier density (AZO $n = 4.4 \times 10^{20} \text{ cm}^{-3}$, BZO $n = 9.2 \times 10^{19} \text{ cm}^{-3}$). (Adapted from [125]) Right: Damp heat stability (85 °C, 85% r.h.) of different, nonencapsulated TCO materials (extracted from [130–132]).

reducing the mobility. Degradation in humid atmosphere is an intrinsic property of ZnO based TCO's and can only be diminished by increasing the layer density [139,140] or by applying proper encapsulation, which includes transparent front sheets with moisture barrier coatings, to prevent humidity exposure of the TCO [141]. Alternative TCO such as fluorine doped tin oxide (FTO), indium tin oxide (ITO) or indium zinc oxide (IZO) could also lead to considerable improvements in damp heat stability [130,131,142] (see Figure 4, right).

While sputtering or chemical vapor deposition are the most common deposition methods for the TCO, solution processed ZnO TCO's have been successfully applied on CIGS by chemical bath deposition [143], electrodeposition [144], and spray pyrolysis [145] but so far without meeting the performance and stability of sputtered reference cells. The major challenge for those processes lies in the fact that the deposition and/or subsequent annealing temperature should not exceed $\sim 200^\circ\text{C}$ at any process step [143].

3. CONCEPTS FOR HIGH EFFICIENCY DEVICES

Device concepts for achieving higher efficiency than in the single junction case include tandem (multi-junction) approaches and illumination under concentrated light. Such concepts for III-V solar cells are well developed, but their application for CIGS solar cells is still in an early stage. From an application point of view, it is also interesting to improve the performance at low light irradiation and we will discuss this in the next sections.

3.1. Tandem solar cells

In order to reduce thermalization losses, or for better utilization of the solar spectrum, two or more solar cells of different bandgap are used in tandem solar cells as to reach higher PV conversion efficiency [146]. With ideally

matched energy bandgaps, the theoretical conversion efficiency limit (detailed balance) under AM1.5G increases from $\sim 33\%$ for single junction to $\sim 45\%$ for dual junction solar cells [147]. Compared with single-crystalline wafer-based solar cells, where this concept has already been successfully applied, tandem devices based on all thin-film polycrystalline layers can profit from reduced complexity and therefore increased market potential. In this paragraph, we review the current state of chalcogenide based on all thin-film tandem devices. The bandgap variability in the chalcopyrite (CIGS) materials system opens an attractive option for tandem cells. For example, CIS or CIGS cells with a bandgap of 1 to 1.1 eV are suitable as a bottom cell in combination with a top cell of bandgap $> 1.6\text{--}1.7\text{ eV}$. Unfortunately, CIGS cells with high bandgap suffer from poor electric properties and high sub-bandgap absorption. Therefore, alternative absorbers such as dye-sensitized solar cells, cadmium telluride or perovskites have been applied as top cells [148–152] to investigate the feasibilities. The cells can be connected independently (4-terminal configuration, Figure 5) or in series (2-terminal configuration), while the latter can be realized by monolithic cell interconnection or by string wise interconnection. A scanning electron microscope cross-section of a 2-terminal monolithic tandem cell is shown in Figure 6. The best efficiencies published for this kind of device so far are 13.0% for a CIGS/dye-sensitized solar cells [151] and 10.9% for a CIGS/perovskite [150] device. While the 2-terminal concept has the advantages of reduced material usage, lower parasitic losses due to the reduced number of TCOs and the use of a single electric circuit, it has the disadvantages of needing current matching between the sub-cells, the requirement for a stable and efficient tunnel/recombination layer and the need for a bottom cell that's stable to the top cell deposition process.

While no efficiencies beyond the single junction record have been published so far, the improvements relative to the sub-cell properties shown in for example,

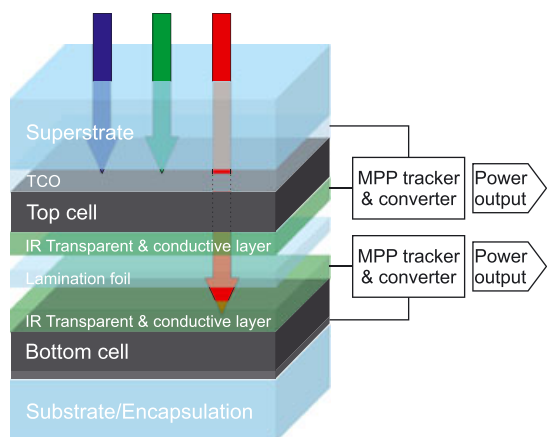


Figure 5. Schematic structure of a 4-terminal tandem structure. CIGS thin film solar cells are a suitable candidate for bottom cell while further research is required to find a suitable top cell.

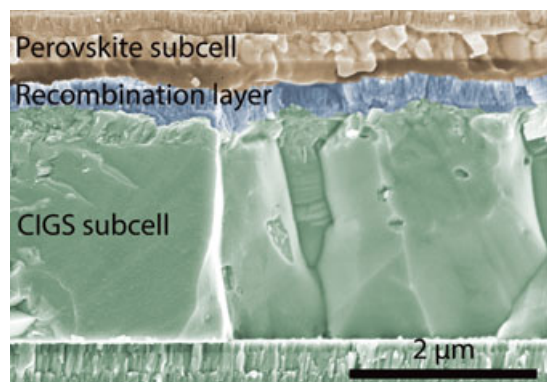


Figure 6. Scanning electron microscope cross-section of a monolithic perovskite/CIGS tandem device with both cells and the recombination layer highlighted in color.

Figure 7 prove the validity of the concept [149,153,154] but obviously further research and development is needed.

3.2. Concentrator operation

Concentrator concepts have been shown in III-V solar cells very successfully [155]. CIGS solar cells are mainly considered for low concentrator applications, reaching 23.3% efficiency at 14.7 suns concentration so far [29]. Higher concentrations could be used when going for microcells, because both resistive losses and temperature increase are strongly reduced [156].

3.3. Low light behavior

Efficiency values for record devices are usually claimed for standard test conditions under AM1.5G illumination.

However, good performance under low light conditions is also important to ensure lower levelized cost of electricity and for some other applications such as indoor energy generation. CIGS solar cell technology shows good performance under low light conditions compared with other technologies [4]. In Figure 8, we show the distribution of solar energy irradiated at different intensity levels on the example of Zuerich (Switzerland). The high fraction of energy received at low energy densities (more than 10% below 10 mW/cm^2) means that an efficiency reduction of only 10% under this irradiation can lead to total efficiency loss in the 1% range. Moreover, CIGS solar cells can also be used for indoor and portable electronics applications. Good performance under such conditions requires high parallel resistances (R_p) [157]. The curves in Figure 8 compare the efficiency of a device with $R_p \sim 10 \text{ k}\Omega \text{ cm}^2$ (black) and $R_p \sim 20 \text{ k}\Omega \text{ cm}^2$ (red). The resulting efficiency increase for light intensities below 1 mW/cm^2 is in the 50% (relative) range. This improvement would already lead to a change in annual power output from 177 kWh/m^2 to 186 kWh/m^2 , which gives an increase of effective efficiency of 0.7% absolute (assuming a global irradiation of 1228 kWh and a distribution as given in Figure 8; the efficiency for each intensity level is averaged over the respective range and corrected for the spectral mismatch between AM1.5G and the LED test setup). The global irradiance for this experiment was measured in 10-min intervals and the average distribution was obtained by evaluating a 10 year time series. The low light efficiencies were measured under white LED irradiation and light levels were measured simultaneously with a thermopile sensor and a lux-meter.

The parallel resistance of CIGS solar cells has been reported to be influenced by localized hotspots [158,159], the window layer properties [157], the absorber composition, especially Cu content [160,161], and the laser scribing parameters [162–165]. These investigations show that CIGS solar cells can be optimized for efficient low light performance.

4. FLEXIBLE CIGS SOLAR CELL APPLICATIONS

CIGS thin film technology has been mostly developed on glass substrates, and for a long time CIGS solar cells deposited on flexible substrates such as plastic film or metal foil could not reach similar efficiencies. Limitations due to impurity diffusions or the need for lower growth temperature imposed by the choice of the substrate were reasons for such efficiency gap. Recent developments [47] however showed that those challenges can be overcome and is best exemplified with an efficiency above 20% achieved on polyimide (PI) foil (Table I). Deposition on a flexible substrate has advantages not only for manufacturing (large area roll-to-roll deposition is possible) but also opens up a whole new field for solar modules designs and applications. Especially, flexible and lightweight CIGS solar

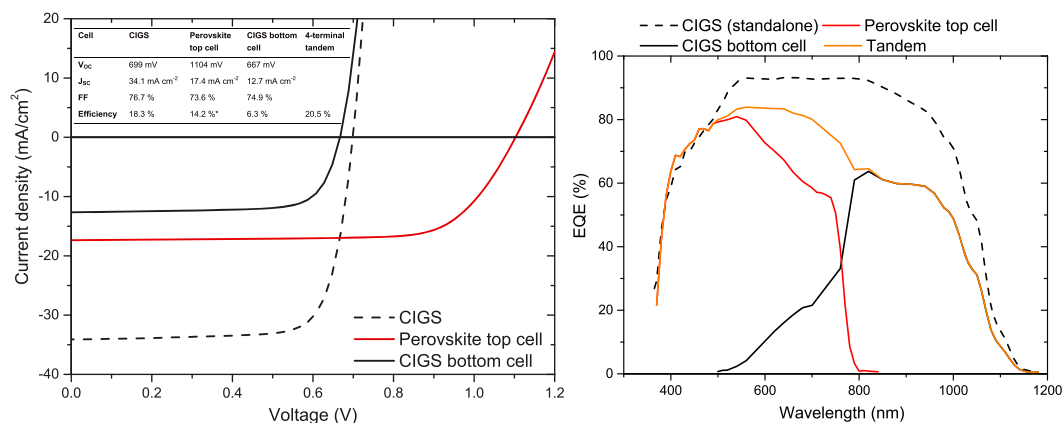


Figure 7. IV and external quantum efficiency (EQE) curves of the highest reported 4-terminal CIGS tandem. *The perovskite efficiency is measured by maximum power point tracking to exclude hysteresis effects [153].

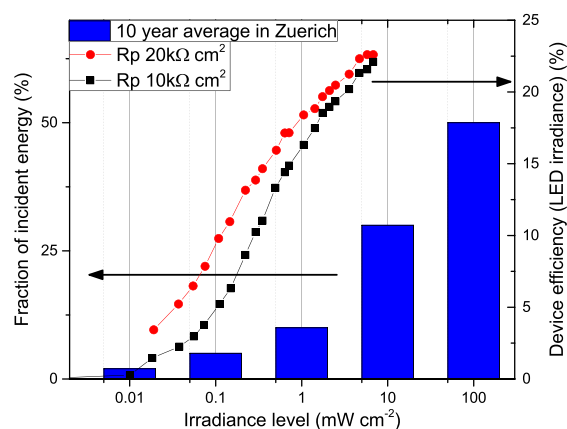


Figure 8. Distribution of incident energy at different irradiance levels on a 10-year average, data measured in Zurich (Switzerland). The curves show the efficiency of CIGS solar cells with different parallel resistances under LED irradiation for application under low light or indoor illumination. The cell area for these devices was 0.27 cm².

modules enable novel applications and concepts for solar electricity generation. Flexibility in shape, power rating, and form factor are some of the advantages that allow clear differentiation from traditional rigid and heavy PV technology, opening the doors to BIPV and transport-integrated PV markets. Table I contains several companies which are active in this domain and offer this type of products or focus on mobile and fast-deployable off-grid solar solutions. As an example, Figure 9 shows potential products based on the module technology of Flisom AG. Beside full flexible solar modules, BIPV solutions can be provided by laminating lightweight solar modules directly onto metallic building elements. Significant reduction of Balance of System costs (BOS), transport, and installation cost can be expected compared with conventional glass-glass

technologies. In the following, we discuss in more detail two applications where lightweight is advantageous, namely space applications and tracking.

4.1. Space applications

Future satellite power subsystem will be designed to achieve higher power level, power densities (kW/kg), launch packaging densities (kW/m³), and lower unit costs (\$/kW) than can be achieved with current solar array technologies. Flexible CIGS solar cells offer the potential for providing very high power levels in a lightweight configuration that can be compactly packaged for launch.

For example, a 3 μ m CIGS PV film (including front and back contact) grown on 25 μ m PI substrate can achieve a specific power of ~ 4 kW/kg (with a conversion efficiency of 15%). This value is potentially more than one order of magnitude above conventional solutions [166]. However, a PI substrate does not offer sufficient mechanical support for deployment; therefore, a supporting back-sheet is needed. Further, a front side encapsulation must be applied in order to protect against mechanical scratches and space environment. Both additional layers do significantly add up to the weight of the module. If relatively dense materials such as glass and steel are used as mechanical support, substrate or encapsulation, respectively, the specific power gets drastically reduced. In Table IV, some indicative numbers are summed up to give a range of what specific power can be achieved in different configurations. The options of using a 50 μ m fluorinated ethylene propylene front laminate [167] or glass are included. If a carbon fiber reinforced plastic or titanium is used as lightweight support, a power density of 0.3–0.5 kW/kg seems achievable. If 100 μ m steel is used as substrate and support the specific power drops to ~ 0.2 kW/kg, the estimation made here is consistent with the estimation of Dhere *et al.* [168].

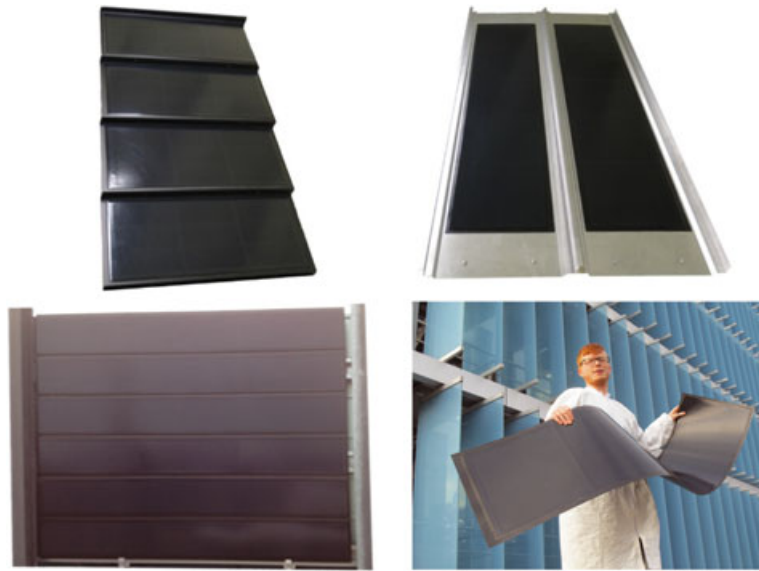


Figure 9. Building-integrated photovoltaic product concepts based on flexible, lightweight monolithic CIGS solar modules on polyimide, from top left to bottom left: residential roof tile, architectural standing seam roof, and metal façade cladding elements. Bottom right: fully rollable module for application on rooftop membrane. All images courtesy of Flisom AG.

Table IV. Estimated specific power of a flexible CIGS thin film module assuming different substrate, support, and front-encapsulation materials.

Substrate + mechanical support		CIGS PV cell	Front encapsulation	Sum	Power/weight ratio at 15% eff. in space
	g/m ²	g/m ²	(50 µm) g/m ²	g/m ²	(1360 W/m ²) kW/kg
PI 25 µm	35	15	None	50	4.1
PI 25 µm + CFRP 200 µm	35 + 320	15	110 (FEP)	470	0.43
Titanium 100 µm	450			565	0.36
Steel 100 µm	780			895	0.23
Steel 100 µm	780	15	125 (Glass)	920	0.22
Steel 127 µm			None	1000	0.20 [168]

CFRP, carbon fiber reinforced plastic; FEP, fluorinated ethylene propylene.

In terms of radiation hardness, CIGS was found to be even superior to GaAs [169]. The bandgap of high efficiency (20%) flexible CIGS is around 1.1 eV [32]. However, a higher bandgap around 1.5 eV would not only be favorable to match the AM0 spectra but also to achieve a smaller temperature coefficient, as a module in space might reach temperatures up to ~150 °C [169], but this has not yet been realized with comparable efficiency. A recent study confirmed the feasibility of the concept of a rollable blanket with integrated flexible CIGS submodules [170].

4.2. Tracking

Optimization of thin film solar modules for usage on PV trackers has lately re-appeared as a topic of interest in utility scale PV markets. First Solar announced during its

Annual Analyst Day in 2016 [171] that its Series 5 module will be introduced to market in a three module configuration for fast installation in single axis tracker systems. This should contribute to reducing BOS costs of such systems significantly. The lightweight design of flexible solar modules has the additional advantage that the required tracker structures for utility PV systems could be considerably lighter and more cost effective. First concepts such as adaptive solar façade [172] or a moisture sensitive wooden-bilayers tracker [173] have been demonstrated employing lightweight modules.

4.3. Manufacturing technology

The transfer of the lab-scale processes into an industrial environment encounters challenges. Several aspects need to be controlled to ensure manufacturing of modules with

acceptable efficiency and production yield. Not only material and process-related issues need to be solved but also engineering of new equipment machines and development of *in situ* process control techniques are required. Industrial production of CIGS solar modules on glass substrates has advanced to high volumes by companies such as Solar Frontier, AVANCIS, Solibro, Manz, and others. However, the manufacturing of flexible CIGS solar cells and modules is relatively less mature despite decent cell efficiencies have been achieved on small area devices in laboratories (Tables I and II). Flexible substrates allow the use of roll-to-roll deposition techniques, as used in the packaging industry, with the potential advantage of high throughput and compact equipment dimensions for each layer of the solar module stack. For the CIGS absorber deposition by co-evaporation or sputtering, evaporation sources and targets need to be positioned in such a way as to reproduce the CIGS growth conditions from the static processes developed on laboratory scale. Adequate *in situ* process control techniques are necessary to ensure stable absorber quality during the continuous deposition onto the moving substrate. As there is a lack of reliable

providers for CIGS roll-to-roll deposition equipment, companies such as Flisom have developed custom solutions.

Figure 10 shows I-V and EQE curve of a 16.0% solar cell based on a CIGS absorber grown by roll-to-roll low-temperature co-evaporation onto a flexible PI foil. The best corresponding mini-module ($5 \times 5 \text{ cm}^2$, 8 cells monolithically connected by laser scribing) achieved an efficiency of 14.3%. The scanning electron microscope cross-section shows an absorber microstructure with large grains, with a TCO deposited in a roll-to-roll process. Further improvements, not only of CIGS growth conditions but also in overall stack and module design, are still required to reach similar efficiency values as reported on laboratory scale for a similar process (e.g., 16.9% for monolithic CIGS on PI [11]). Those results, together with results reported on stainless steel (e.g., MiaSolé with 16.5% efficiency [18] and Global Solar with 14.7% (presented at IW-CIGSTech 7) on module size or 17% on 6" cells from Midsummer [19]) show that module manufacturing on flexible substrate is on a good path to be cost-competitive in a near future.

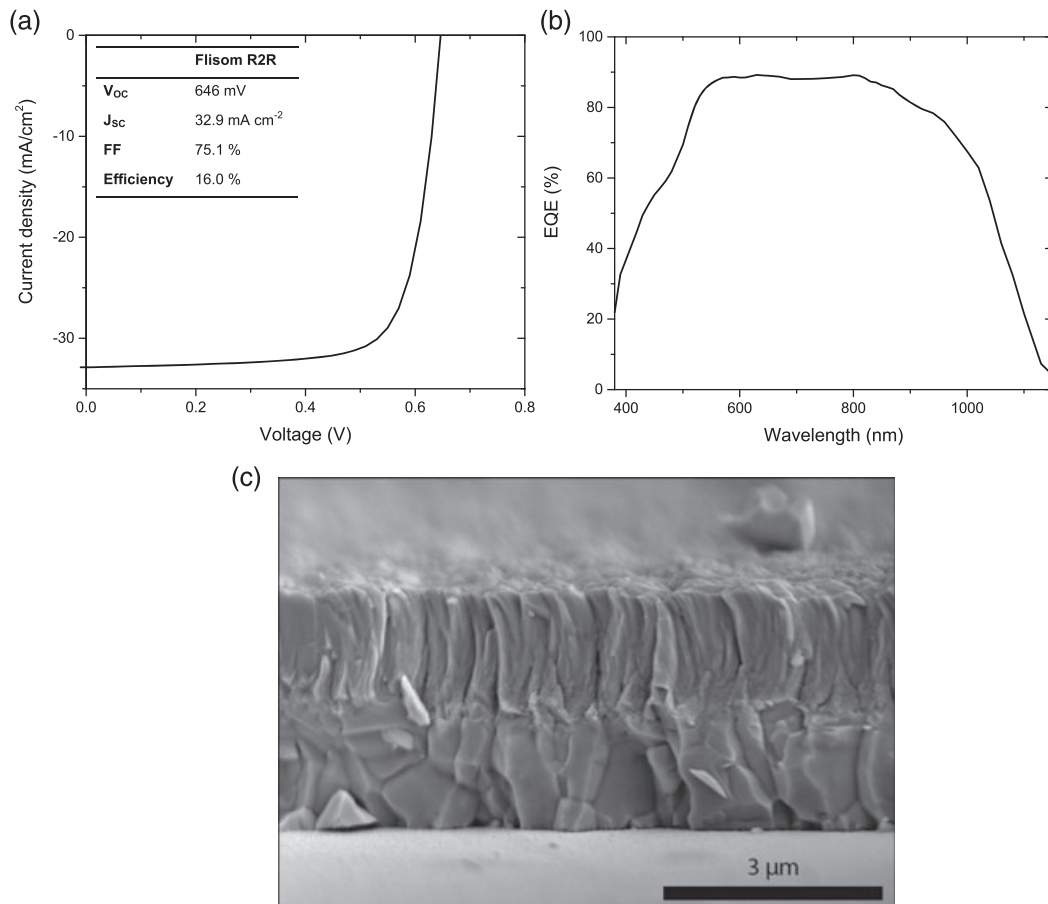


Figure 10. (a) IV and (b) external quantum efficiency (EQE) curves of a solar cell based on a CIGS absorber deposited in a roll-to-roll process. Inset shows the IV parameters. (c) Scanning electron microscope cross section of a fully roll-to-roll processed solar cell.

5. CONCLUSIONS AND PROSPECTS

The application of alkali PDT by several laboratories around the world has been one of the main trigger for the quick progress of record efficiencies observed over the past couple of years. Alternative buffer layers, especially based on Zn (O, OH, S) and TCOs have yielded remarkably high efficiency and stable performance.

It will however take some time to fully translate those new developments into industrial production. Considering the significant and fast improvements observed on lab scale, it is likely that this new knowledge will contribute greatly in increasing the performance of industrial CIGS modules in the near future. Moreover, the large scale production of solar modules on flexible substrate gives the opportunity for differentiated products, applicable where traditional rigid heavy modules have some limitations. Flexible lightweight solar modules will find their application and growth, especially for BIPV.

The combination of CIGS with wide bandgap perovskite shows interesting options for tandem solar cells; however, further research is needed to enhance device efficiency. CIGS solar cell processing can further be optimized, for example, to enhance parallel resistance in order to make them more efficient in low light applications.

ACKNOWLEDGEMENTS

This work was partially supported by the Swiss State Secretariat for Education, Research and Innovation (SERI) under contract number REF-1131-52107, the National Research Programm 'Energy Turnaround' (NRP 70) of the Swiss National Science Foundation (SNSF) in the project PV2050, the Swiss National Science Foundation (grant numbers 20NA21_150950 and 200021_149453/1), the Swiss Federal Office of Energy (grant numbers SI/501145-01 and SI/501072-01), and the Competence Center for Energy & Mobility (CCEM) project 906_CON-NECT PV.

The authors would like to acknowledge the Swiss National Air Pollution Monitoring Network NABEL (BAFU and Empa) for the global irradiation data.

REFERENCES

1. Jackson P, Wuerz R, Hariskos D, Lotter E, Witte W, Powalla M. Effects of heavy alkali elements in Cu(In, Ga)Se₂ solar cells with efficiencies up to 22.6%. *physica status solidi (RRL) – Rapid Research Letters* 2016. DOI:10.1002/pssr.201600199
2. Makrides G, Zinsser B, Norton M, Georgiou GE, Schubert M, Werner JH. Potential of photovoltaic systems in countries with high solar irradiation. *Renewable and Sustainable Energy Reviews* 2010; **14**(2): 754–762. DOI:10.1016/j.rser.2009.07.021
3. Bhandari KP, Collier JM, Ellingson RJ, Apul DS. Energy payback time (EPBT) and energy return on energy invested (EROI) of solar photovoltaic systems: A systematic review and meta-analysis. *Renewable and Sustainable Energy Reviews* 2015; **47**: 133–141. DOI:10.1016/j.rser.2015.02.057
4. CIS advantages in real-world conditions. Solar Frontier company webpage Accessed May 23, 2016. <http://www.solar-frontier.com/eng/technology/Performance/index.html>.
5. CIGS white paper initiative – CIGS thin-film photovoltaics. CIGS White Paper Initiative Accessed May 14, 2016. <http://cigs-pv.net/cigs-white-paper-initiative/>.
6. Reinhard P, Buecheler S, Tiwari AN. Technological status of Cu(In,Ga)(Se,S)₂-based photovoltaics. *Solar Energy Materials and Solar Cells* 2013; **119**: 287–290. DOI:10.1016/j.solmat.2013.08.030
7. 16 percent: Manz achieves new world record for efficiency of CIGS thin-film solar modules | Manz AG. Accessed May 12, 2016. <http://www.manz.com/>.
8. Green MA, Emery K, Hishikawa Y, Warta W, Dunlop ED. Solar cell efficiency tables (version 47). *Progress in Photovoltaics: Research and Applications* 2016; **24**(1): 3–11. DOI:10.1002/pip.2728
9. Hanergy analysts report. hanergythinfilmpower. Accessed May 12, 2016. <http://www.hanergythinfilmpower.com/admin/media/anaytsts-report/20131121-quam-research-hanergy-solar-group--0566-hk-.pdf>.
10. Siva Power approaches 19% efficiency in record time; Adds to Solar Company's Powerful Technical Advisory Board. Accessed May 12, 2016. <http://www.prnewswire.com/news-releases/siva-power-approaches-19-efficiency-in-record-time-adds-to-solar-companys-powerful-technical-advisory-board-243722021.html>.
11. Reinhard P, Pianezzi F, Bissig B, Chirila A, Blosch P, Nishiwaki S, Buecheler S, Tiwari AN. Cu (In,Ga)Se thin-film solar cells and modules - a boost in efficiency due to Potassium. *IEEE Journal of Photovoltaics* 2015; **5**(2): 656–663. DOI:10.1109/JPHOTOV.2014.2377516
12. Wiedeman S, Albright S, Britt JS, Schoop U, Schuler S, Stoss W, Verebelyi D. Manufacturing ramp-up of flexible CIGS PV. In *2010 35th IEEE Photovoltaic Specialists Conference (PVSC)*, 2010; 003485–003490. DOI: 10.1109/PVSC.2010.5614725
13. Ascent Solar - Ascent Solar achieves 14 percent cell efficiency milestone in commercial production - October 21, 2009. October 21, 2009. Accessed May 12, 2016.

- <http://investors.ascentsolar.com/releasedetail.cfm?ReleaseID=437180>.
14. Kushiya K. CIS-based thin-film PV technology in solar frontier K.K. *Solar Energy Materials and Solar Cells* 2014; **122**: 309–313. DOI:10.1016/j.solmat.2013.09.014
 15. Solar Frontier achieves world record thin-film solar cell efficiency: 22.3%. Solar Frontier company webpage. December 8, 2015 Accessed April 25, 2016. <http://www.solar-frontier.com/eng/news/2015/C051171.html>.
 16. Nakamura M, Chiba Y, Kijima S, Horiguchi K, Yanagisawa Y, Sawai Y, Ishikawa K, Hakuma H. Achievement of 17.5% efficiency with 30 #x00D7; 30 cm²-sized Cu(In,Ga)(Se,S)₂ submodules. In *2012 38th IEEE Photovoltaic Specialists Conference (PVSC)*, 2012; 001807–001810. DOI: 10.1109/PVSC.2012.6317944
 17. AVANCIS erzielt erneuten Wirkungsgradrekord: Fraunhofer ISE zertifiziert CIGS-Solarmodul mit Wirkungsgrad von 17,9 %. AVANCIS Advanced Solar Power May 2, 2016. Accessed May 9, 2016. <http://www.avancis.de/footer/presse/newsansicht/article/avancis-erzielt-erneuten-wirkungsgradrekord-fraunhofer-ise-zertifiziert-cigs-solarmodul-mit-wirkungsgrad-von-179.html>.
 18. MiaSolé - Home. MiaSolé. Accessed May 12, 2016. <http://miasole.com/>.
 19. Technology - Midsummer. Accessed May 12, 2016. <http://midsummer.se/technology>.
 20. WonCIGS current status. Accessed May 12, 2016. http://www.woncigs.com/bbs/content.php?co_id=Current.
 21. NuvoSun™ FlexsoLyt™ | Dow. DOW solar NuvoSun. Accessed May 12, 2016. <http://www.dowsolar.com/en/nuvosun/nuvosun-lightweight-flexible>.
 22. HULKet Energy takes CIGS module power to record 324 watts. HULKet Energy Corporation July 7, 2015 Accessed May 14, 2016. <http://www.hulket.com/?p=4277>.
 23. Stion Demonstrates 23.2% efficiency thin film with simply better tandem technology. Stion. Accessed May 2, 2016. <http://www.stion.com/stion-demonstrates-23-2-efficiency-thin-film-with-simply-better-tandem-technology/>.
 24. Broussillou C, Viscogliosi C, Rogee A, Angle S, Grand PP, Bodnar S, Debauche C, Allary JL, Bertrand B, Guillou C, Parissi L, Coletti S. Statistical process control for Cu(In,Ga)(S,Se)₂ electrodeposition-based manufacturing process of 60x120cm² modules up to 14,0% efficiency. In *Photovoltaic Specialist Conference (PVSC), 2015 IEEE 42nd*, 2015; 1–5. DOI: 10.1109/PVSC.2015.7356224
 25. Aksu S, Pethe S, Kleiman-Shwarscstein A, Kundu S, Pinarbasi M. Recent advances in electroplating based CIGS solar cell fabrication. In *2012 38th IEEE Photovoltaic Specialists Conference (PVSC)*, 2012; 003092–003097. DOI: 10.1109/PVSC.2012.6318235
 26. Powalla M, Witte W, Jackson P, Paetel S, Lotter E, Wuerz R, Kessler F, Tschamber C, Hempel W, Hariskos D, Menner R, Bauer A, Spiering S, Ahlswede E, Friedlmeier TM, Blázquez-Sánchez D, Klugius I, Wischmann W. CIGS Cells and Modules With High Efficiency on Glass and Flexible Substrates. *IEEE Journal of Photovoltaics* 2014; **4**(1): 440–446. DOI:10.1109/JPHOTOV.2013.2280468
 27. Friedlmeier TM, Jackson P, Bauer A, Hariskos D, Kiowski O, Wuerz R, Powalla M. Improved photocurrent in Cu(In,Ga)Se₂ solar cells: from 20.8% to 21.7% efficiency with CdS buffer and 21.0% Cd-free. *IEEE Journal of Photovoltaics* 2015; **5**(5): 1487–1491. DOI:10.1109/JPHOTOV.2015.2458039
 28. Hariskos D, Fuchs B, Menner R, Naghavi N, Hubert C, Lincot D, Powalla M. The Zn(S,O,OH)/ZnMgO buffer in thin-film Cu(In,Ga)(Se,S)₂-based solar cells part II: magnetron sputtering of the ZnMgO buffer layer for in-line co-evaporated Cu(In,Ga)Se₂ solar cells. *Progress in Photovoltaics: Research and Applications* 2009; **17**(7): 479–488. DOI:10.1002/pip.897
 29. Ward JS, Egaas B, Noufi R, Contreras M, Ramanathan K, Osterwald C, Emery K. Cu(In,Ga)Se₂ solar cells measured under low flux optical concentration. In *2014 IEEE 40th Photovoltaic Specialist Conference (PVSC)*, 2014; 2934–2937. DOI: 10.1109/PVSC.2014.6925546
 30. Mansfield LM, Noufi R, Muzzillo CP, DeHart C, Bowers K, To B, Pankow JW, Reedy RC, Ramanathan K. Enhanced performance in Cu(In,Ga)Se solar cells fabricated by the two-step selenization process with a Potassium Fluoride postdeposition treatment. *IEEE Journal of Photovoltaics* 2014; **4**(6): 1650–1654. DOI:10.1109/JPHOTOV.2014.2354259
 31. CIGS solar cell with world's highest level energy conversion efficiency. Toshiba R&D Center. Accessed May 11, 2016. https://www.toshiba.co.jp/rdc/rd/fields/14_e06_e.htm.
 32. Chirilă A, Reinhard P, Pianezzi F, Bloesch P, Uhl AR, Fella C, Kranz L, Keller D, Gretener C, Hagendorfer H, Jaeger D, Erni R, Nishiwaki S, Buecheler S, Tiwari AN. Potassium-induced surface modification of Cu(In,Ga)Se₂ thin films for high-efficiency solar cells. *Nature Materials* 2013; **12**(12): 1107–1111. DOI:10.1038/nmat3789

33. Nishiwaki S, Burn A, Buecheler S, Murralt M, Pilz S, Romano V, Witte R, Krainer L, Spühler GJ, Tiwari AN. A monolithically integrated high-efficiency Cu (In,Ga)Se₂ mini-module structured solely by laser. *Progress in Photovoltaics: Research and Applications* 2015. DOI:10.1002/pip.2583
34. Kamikawa Y, Nishinaga J, Ishizuka S, Shibata H, Niki S. Effects of Mo surface oxidation on Cu(In, Ga)Se₂ solar cells fabricated by three-stage process with KF postdeposition treatment. *Japanese Journal of Applied Physics* 2016; **55**(2): 22304. DOI:10.7567/JJAP.55.022304
35. Moriwaki K, Nomoto M, Yuuya S, Murakami N, Ohgoh T, Yamane K, Ishizuka S, Niki S. Monolithically integrated flexible Cu(In,Ga)Se₂ solar cells and submodules using newly developed structure metal foil substrate with a dielectric layer. *Solar Energy Materials and Solar Cells* 2013; **112**: 106–111. DOI:10.1016/j.solmat.2013.01.016
36. Thompson CP, Chen L, Shafarman WN, Lee J, Fields S, Birkmire RW. Bandgap gradients in (Ag,Cu)(In, Ga)Se₂ thin film solar cells deposited by three-stage co-evaporation. In *Photovoltaic Specialist Conference (PVSC), 2015 IEEE 42nd*, 2015; 1–6. DOI: 10.1109/PVSC.2015.7355692
37. Nakamura M, Kouji Y, Chiba Y, Hakuma H, Kobayashi T, Nakada T. Achievement of 19.7% efficiency with a small-sized Cu(InGa)(SeS)₂ solar cells prepared by sulfurization after selenization process with Zn-based buffer. In *2013 IEEE 39th Photovoltaic Specialists Conference (PVSC)*, 2013; 0849–0852. DOI: 10.1109/PVSC.2013.6744278
38. Kobayashi T, Yamaguchi H, Nakada T. Effects of combined heat and light soaking on device performance of Cu(In,Ga)Se₂ solar cells with ZnS(O,OH) buffer layer. *Progress in Photovoltaics: Research and Applications* 2014; **22**(1): 115–121. DOI:10.1002/pip.2339
39. Haarstrich J, Metzner H, Oertel M, Ronning C, Rissom T, Kaufmann CA, Unold T, Schock HW, Windeln J, Mannstadt W, Rudigier-Voigt E. Increased homogeneity and open-circuit voltage of Cu (In,Ga)Se₂ solar cells due to higher deposition temperature. *Solar Energy Materials and Solar Cells* 2011; **95**(3): 1028–1030. DOI:10.1016/j.solmat.2010.10.021
40. Merdes S, Ziem F, Lavrenko T, Walter T, Lauermaun I, Klingsporn M, Schmidt S, Hergert F, Schlattmann R. Above 16% efficient sequentially grown Cu(In, Ga)(Se,S)₂-based solar cells with atomic layer deposited Zn(O,S) buffers. *Progress in Photovoltaics: Research and Applications* 2015. DOI:10.1002/pip.2579
41. Lindahl J, Zimmermann U, Szaniawski P, Törndahl T, Hultqvist A, Salomé P, Platzer-Björkman C, Edoff M. Inline Cu(In,Ga)Se co-evaporation for high-efficiency solar cells and modules. *IEEE Journal of Photovoltaics* 2013; **3**(3): 1100–1105. DOI:10.1109/JPHOTOV.2013.2256232
42. Wallin E, Malm U, Jarmar T, Lundberg O, Edoff M, Stolt L. World-record Cu(In,Ga)Se₂-based thin-film sub-module with 17.4% efficiency. *Progress in Photovoltaics: Research and Applications* 2012; **20**(7): 851–854. DOI:10.1002/pip.2246
43. Nam J, Kang Y, Lee D, Yang J, Kim Y-S, Mo CB, Park S, Kim D. Achievement of 17.9% efficiency in 30 × 30 cm² Cu(In,Ga)(Se,S)₂ solar cell sub-module by sulfurization after selenization with Cd-free buffer. *Progress in Photovoltaics: Research and Applications* 2016; **24**(2): 175–182. DOI:10.1002/pip.2653
44. Bhattacharya RN. CIGS-based solar cells prepared from electrodeposited stacked Cu/In/Ga layers. *Solar Energy Materials and Solar Cells* 2013; **113**: 96–99. DOI:10.1016/j.solmat.2013.01.028
45. Todorov TK, Gunawan O, Gokmen T, Mitzi DB. Solution-processed Cu(In,Ga)(S,Se)₂ absorber yielding a 15.2% efficient solar cell. *Progress in Photovoltaics: Research and Applications* 2013; **21**(1): 82–87. DOI:10.1002/pip.1253
46. Otte K, Makhova L, Braun A, Kononov I. Flexible Cu(In,Ga)Se₂ thin-film solar cells for space application. *Thin Solid Films* 2006; **511–512**: 613–622. DOI:10.1016/j.tsf.2005.11.068
47. Reinhard P, Chirilă A, Blösch P, Pianezzi F, Nishiwaki S, Buecheler S, Tiwari AN. Review of Progress Toward 20% Efficiency Flexible CIGS Solar Cells and Manufacturing Issues of Solar Modules. *IEEE Journal of Photovoltaics* 2013; **3**(1): 572–580. DOI:10.1109/JPHOTOV.2012.2226869
48. Shafarman WN, Siebentritt S, Stolt L. Cu(InGa)Se₂ solar cells. In *Handbook of Photovoltaic Science and Engineering*, Luque A, Hegedus S (eds). John Wiley & Sons, Ltd, Chichester, UK, 2010. 546–599.
49. Scheer R, Schock H-W. *Chalcogenide Photovoltaics: Physics, Technologies, and Thin Film Devices*. : Wiley, Weinhei, Germany, 2011.
50. NREL: National Center for Photovoltaics Home Page. Accessed April 27, 2016. <http://www.nrel.gov/ncpv/>.
51. Jackson P, Hariskos D, Wuerz R, Kiowski O, Bauer A, Friedlmeier TM, Powalla M. Properties of Cu(In, Ga)Se₂ solar cells with new record efficiencies up to 21.7%. *physica status solidi (RRL) – Rapid Research Letters* 2015; **9**(1): 28–31. DOI:10.1002/pssr.201409520

52. Fortunato E, Ginley D, Hosono H, Paine DC. Transparent conducting oxides for photovoltaics. *MRS Bulletin* 2007; **32**(3): 242–247. DOI:10.1557/mrs2007.29
53. Rau U, Grabitz PO, Werner JH. Resistive limitations to spatially inhomogeneous electronic losses in solar cells. *Applied Physics Letters* 2004; **85**(24): 6010–6012. DOI:10.1063/1.1835536
54. Naghavi N, Abou-Ras D, Allsop N, Barreau N, Bücheler S, Ennaoui A, Fischer C-H, Guillen C, Hariskos D, Herrero J, Klenk R, Kushiya K, Lincot D, Menner R, Nakada T, Platzer-Björkman C, Spiering S, Tiwari AN, Törndahl T. Buffer layers and transparent conducting oxides for chalcopyrite Cu(In,Ga)(S,Se)₂ based thin film photovoltaics: present status and current developments. *Progress in Photovoltaics: Research and Applications* 2010; **18**(6): 411–433. DOI:10.1002/pip.955
55. Hedstrom J, Ohlsen H, Bodegard M, Kylner A, Stolt L, Hariskos D, Ruckh M, Schock HW. ZnO/CdS/Cu(In,Ga)Se₂ thin-film solar-cells with improved performance. *Conference Record of the Twenty Third IEEE Photovoltaic Specialists Conference - 1993* 1993; 364–371. DOI:10.1109/Pvsc.1993.347154
56. Rudmann D, Brémaud D, da Cunha AF, Bilger G, Strohm A, Kaelin M, Zogg H, Tiwari AN. Sodium incorporation strategies for CIGS growth at different temperatures. *Thin Solid Films* 2005; **480–481**: 55–60. DOI:10.1016/j.tsf.2004.11.071
57. Rudmann D, da Cunha AF, Kaelin M, Kurdesau F, Zogg H, Tiwari AN, Bilger G. Efficiency enhancement of Cu(In,Ga)Se₂ solar cells due to post-deposition Na incorporation. *Applied Physics Letters* 2004; **84**(7): 1129–1131. DOI: doi:10.1063/1.1646758
58. Reinhard P, Bissig B, Pianezzi F, Avancini E, Hagendorfer H, Keller D, Fuchs P, Döbeli M, Vigo C, Crivelli P, Nishiwaki S, Buecheler S, Tiwari AN. Features of KF and NaF postdeposition treatments of Cu(In,Ga)Se₂ absorbers for high efficiency thin film solar cells. *Chemistry of Materials* 2015. DOI:10.1021/acs.chemmater.5b02335
59. Laemmle A, Wuerz R, Powalla M. Efficiency enhancement of Cu(In,Ga)Se₂ thin-film solar cells by a post-deposition treatment with potassium fluoride. *physica status solidi (RRL) – Rapid Research Letters* 2013; **7**(9): 631–634. DOI:10.1002/pssr.201307238
60. Jackson P, Hariskos D, Wuerz R, Kiowski O, Bauer A, Powalla M. Properties of high efficiency Cu(In,Ga)Se₂ solar cells. In *MRS Spring Meeting & Exhibit, San Francisco B*, vol 7, 2015.
61. Jackson P, Hariskos D, Wuerz R, Wischmann W, Powalla M. Compositional investigation of potassium doped Cu(In,Ga)Se₂ solar cells with efficiencies up to 20.8%. *physica status solidi (RRL) – Rapid Research Letters* 2014; **8**(3): 219–222. DOI:10.1002/pssr.201409040
62. Herrmann D, Kratzert P, Weeke S, Zimmer M, Djordjevic-Reiss J, Hunger R, Lindberg P, Wallin E, Lundberg O, Stolt L. CIGS module manufacturing with high deposition rates and efficiencies. In *2014 IEEE 40th Photovoltaic Specialist Conference (PVSC)*, 2014; 2775–2777. DOI: 10.1109/PVSC.2014.6925505
63. Reinhard P, Bissig B, Pianezzi F, Hagendorfer H, Sozzi G, Menozzi R, Gretener C, Nishiwaki S, Buecheler S, Tiwari AN. Alkali-templated surface nanopatterning of chalcogenide thin films: a novel approach toward solar cells with enhanced efficiency. *Nano Letters* 2015; **15**(5): 3334–3340. DOI:10.1021/acs.nanolett.5b00584
64. Wei S-H, Zhang SB, Zunger A. Effects of Na on the electrical and structural properties of CuInSe₂. *Journal of Applied Physics* 1999; **85**(10): 7214–7218. DOI:10.1063/1.370534
65. Contreras M, Tuttle J, Du D, Qi Y, Swartzlander A, Tennant A, Noufi R. Graded band-gap Cu(In,Ga)Se₂ thin-film solar cell absorber with enhanced open-circuit voltage. *Applied Physics Letters* 1993; **63**(13): 1824–1826. DOI:10.1063/1.110675
66. Gabor AM, Tuttle JR, Albin DS, Contreras MA, Noufi R, Hermann AM. High-efficiency CuIn_xGa_{1-x}Se₂ solar cells made from (In_xGa_{1-x})₂Se₃ precursor films. *Applied Physics Letters* 1994; **65**(2): 198–200. DOI:10.1063/1.112670
67. Marudachalam M, Birkmire RW, Hichri H, Schultz JM, Swartzlander A, Al-Jassim MM. Phases, morphology, and diffusion in CuIn_xGa_{1-x}Se₂ thin films. *Journal of Applied Physics* 1997; **82**(6): 2896–2905. DOI:10.1063/1.366122
68. Witte W, Abou-Ras D, Albe K, Bauer GH, Bertram F, Boit C, Brüggemann R, Christen J, Dietrich J, Eicke A, Hariskos D, Maiberg M, Mainz R, Meessen M, Müller M, Neumann O, Orgis T, Paetel S, Pohl J, Rodriguez-Alvarez H, Scheer R, Schock H-W, Unold T, Weber A, Powalla M. Gallium gradients in Cu(In,Ga)Se₂ thin-film solar cells. *Progress in Photovoltaics: Research and Applications* 2015; **23**(6): 717–733. DOI:10.1002/pip.2485
69. Seyrling S, Chirila A, Güttler D, Pianezzi F, Rossbach P, Tiwari AN. Modification of the three-stage evaporation process for CuIn_{1-x}Ga_xSe₂ absorber deposition. *Thin Solid Films* 2011; **519**(21): 7232–7236. DOI:10.1016/j.tsf.2010.12.146
70. Reinhard P, Pianezzi F, Kranz L, Nishiwaki S, Chirilă A, Buecheler S, Tiwari AN. Flexible Cu

- (In,Ga)Se₂ solar cells with reduced absorber thickness. *Progress in Photovoltaics: Research and Applications* 2015; **23**(3): 281–289. DOI:10.1002/pip.2420
71. Szaniawski P, Salomé P, Fjällström V, Törndahl T, Zimmermann U, Edoff M. Influence of varying Cu content on growth and performance of Ga-graded Cu(In,Ga)Se₂ solar cells. *IEEE Journal of Photovoltaics* 2015; **5**(6): 1775–1782. DOI:10.1109/JPHOTOV.2015.2478033
 72. Bissig B, Reinhard P, Pianezzi F, Hagendorfer H, Nishiwaki S, Buecheler S, Tiwari AN. Effects of NaF evaporation during low temperature Cu(In,Ga)Se₂ growth. *Thin Solid Films* 2015; **582**: 56–59. DOI:10.1016/j.tsf.2014.11.026
 73. Salomé PMP, Rodriguez-Alvarez H, Sadewasser S. Incorporation of alkali metals in chalcogenide solar cells. *Solar Energy Materials and Solar Cells* 2015; **143**: 9–20. DOI:10.1016/j.solmat.2015.06.011
 74. Rudmann D, Brémaud D, Zogg H, Tiwari AN. Na incorporation into Cu(In,Ga)Se₂ for high-efficiency flexible solar cells on polymer foils. *Journal of Applied Physics* 2005; **97**(8): 84903. DOI:10.1063/1.1857059
 75. Nishiwaki S, Satoh T, Hashimoto Y, Negami T, Wada T. Preparation of Cu(In,Ga)Se₂ thin films at low substrate temperatures. *Journal of Materials Research* 2001; **16**(2): 394–399. DOI:10.1557/JMR.2001.0059
 76. Chirilă A, Buecheler S, Pianezzi F, Bloesch P, Gretener C, Uhl AR, Fella C, Kranz L, Perrenoud J, Seyrling S, Verma R, Nishiwaki S, Romanyuk YE, Bilger G, Tiwari AN. Highly efficient Cu(In,Ga)Se₂ solar cells grown on flexible polymer films. *Nature Materials* 2011; **10**(11): 857–861. DOI:10.1038/nmat3122
 77. Dullweber T, Anna GH, Rau U, Schock HW. A new approach to high-efficiency solar cells by band gap grading in Cu(In,Ga)Se₂ chalcopyrite semiconductors. *Solar Energy Materials and Solar Cells* 2001; **67**(1–4): 145–150. DOI:10.1016/S0927-0248(00)00274-9
 78. Niemegeers A, Burgelman M, Herberholz R, Rau U, Hariskos D, Schock H-W. Model for electronic transport in Cu(In,Ga)Se₂ solar cells. *Progress in Photovoltaics: Research and Applications* 1998; **6**(6): 407–421. DOI:10.1002/(SICI)1099-159X(199811/12)6:6<407::AID-PIP230>3.0.CO;2-U
 79. Klenk R. Characterisation and modelling of chalcopyrite solar cells. *Thin Solid Films* 2001; **387**(1–2): 135–140. DOI:10.1016/S0040-6090(00)01736-3
 80. Sozzi G, Troni F, Menozzi R. On the combined effects of window/buffer and buffer/absorber conduction-band offsets, buffer thickness and doping on thin-film solar cell performance. *Solar Energy Materials and Solar Cells* 2014; **121**: 126–136. DOI:10.1016/j.solmat.2013.10.037
 81. Gloeckler M, Sites JR. Band-gap grading in Cu(In,Ga)Se₂ solar cells. *Journal of Physics and Chemistry of Solids* 2005; **66**(11): 1891–1894. DOI:10.1016/j.jpcs.2005.09.087
 82. Decock K, Khelifi S, Burgelman M. Analytical versus numerical analysis of back grading in CIGS solar cells. *Solar Energy Materials and Solar Cells* 2011; **95**(6): 1550–1554. DOI:10.1016/j.solmat.2010.10.020
 83. Salomé PMP, Fjällström V, Szaniawski P, Leitão JP, Hultqvist A, Fernandes PA, Teixeira JP, Falcão BP, Zimmermann U, da Cunha AF, Edoff M. A comparison between thin film solar cells made from co-evaporated CuIn_{1-x}Ga_xSe₂ using a one-stage process versus a three-stage process. *Progress in Photovoltaics: Research and Applications* 2015; **23**(4): 470–478. DOI:10.1002/pip.2453
 84. Mainz R, Rodriguez-Alvarez H, Klaus M, Thomas D, Lauche J, Weber A, Heinemann MD, Brunken S, Greiner D, Kaufmann CA, Unold T, Schock H-W, Genzel C. Sudden stress relaxation in compound semiconductor thin films triggered by secondary phase segregation. *Physical Review B* 2015; **92**(15): 155310. DOI:10.1103/PhysRevB.92.155310
 85. Nakada T, Ohbo H, Watanabe T, Nakazawa H, Matsui M, Kunioka A. Improved Cu(In,Ga)(S,Se)₂ thin film solar cells by surface sulfurization. *Solar Energy Materials and Solar Cells* 1997; **49**(1–4): 285–290. DOI:10.1016/S0927-0248(97)00054-8
 86. Ohashi D, Nakada T, Kunioka A. Improved CIGS thin-film solar cells by surface sulfurization using In₂S₃ and sulfur vapor. *Solar Energy Materials and Solar Cells* 2001; **67**(1–4): 261–265. DOI:10.1016/S0927-0248(00)00290-7
 87. Lavrenko T, Ott T, Walter T. Impact of sulfur and gallium gradients on the performance of thin film Cu(In,Ga)(Se,S)₂ solar cells. *Thin Solid Films* 2015; **582**: 51–55. DOI:10.1016/j.tsf.2014.11.024
 88. Kobayashi T, Yamaguchi H, Jehl Li Kao Z, Sugimoto H, Kato T, Hakuma H, Nakada T. Impacts of surface sulfurization on Cu(In_{1-x}Ga_x)Se₂ thin-film solar cells. *Progress in Photovoltaics: Research and Applications* 2015; **23**(10): 1367–1374. DOI:10.1002/pip.2554
 89. Hiroi H, Iwata Y, Adachi S, Sugimoto H, Yamada A. New world-record efficiency for pure-sulfide Cu(In,Ga)S₂ thin-film solar cell with Cd-free buffer layer via KCN-free process. *IEEE Journal of Photovoltaics* 2016; **6**(3): 760–763. DOI:10.1109/JPHOTOV.2016.2537540

90. Witte W, Spiering S, Hariskos D. Substitution of the CdS buffer layer in CIGS thin-film solar cells. *Vakuum in Forschung und Praxis* 2014; **26**(1): 23–27. DOI:10.1002/vipr.201400546
91. Hariskos D, Spiering S, Powalla M. Buffer layers in Cu(In,Ga)Se₂ solar cells and modules. *Thin Solid Films* 2005; **480–481**: 99–109. DOI:10.1016/j.tsf.2004.11.118
92. Wada T, Hayashi S, Hashimoto Y, Nishiwaki S, Sato T, Negami T, Nishitani M. High efficiency Cu (In, Ga) Se₂ (CIGS) solar cells with improved CIGS surface. In *Proceedings of the 2nd World Conference and Exhibition on Photovoltaic Energy Conversion*, 1998; 403–408.
93. Meyer BK, Polity A, Farangis B, He Y, Hasselkamp D, Krämer T, Wang C. Structural properties and bandgap bowing of ZnO_{1-x}S_x thin films deposited by reactive sputtering. *Applied Physics Letters* 2004; **85**(21): 4929–4931. DOI:10.1063/1.1825053
94. Persson C, Platzer-Björkman C, Malmström J, Törndahl T, Edoff M. Strong valence-band offset bowing of ZnO(1-x)S_x enhances p-type Nitrogen doping of ZnO-like alloys. *Physical Review Letters* 2006; **97**(14): 146403. DOI:10.1103/PhysRevLett.97.146403
95. Grimm A, Kieven D, Klenk R, Lauermann I, Neisser A, Niesen T, Palm J. Junction formation in chalcopyrite solar cells by sputtered wide gap compound semiconductors. *Thin Solid Films* 2011; **520**(4): 1330–1333. DOI:10.1016/j.tsf.2011.04.150
96. Naghavi N, Temgoua S, Hildebrandt T, Guillemoles JF, Lincot D. Impact of oxygen concentration during the deposition of window layers on lowering the metastability effects in Cu(In,Ga)Se₂/CBD Zn(S,O) based solar cell. *Progress in Photovoltaics: Research and Applications* 2015; **23**(12): 1820–1827. DOI:10.1002/pip.2626
97. Buffière M, Barreau N, Arzel L, Zabierowski P, Kessler J. Minimizing metastabilities in Cu(In,Ga)Se₂/(CBD)Zn(S,O,OH)/i-ZnO-based solar cells. *Progress in Photovoltaics: Research and Applications* 2015; **23**(4): 462–469. DOI:10.1002/pip.2451
98. Kobayashi T, Kumazawa T, Jehl Li Kao Z, Nakada T. Post-treatment effects on ZnS(O,OH)/Cu(In,Ga)Se₂ solar cells deposited using thioacetamide-ammonia based solution. *Solar Energy Materials and Solar Cells* 2014; **123**: 197–202. DOI:10.1016/j.solmat.2014.01.013
99. Hubert C, Naghavi N, Canava B, Etcheberry A, Lincot D. Thermodynamic and experimental study of chemical bath deposition of Zn(S,O,OH) buffer layers in basic aqueous ammonia solutions. Cell results with electrodeposited CuIn(S,Se)₂ absorbers. *Thin Solid Films* 2007; **515**(15): 6032–6035. DOI:10.1016/j.tsf.2006.12.139
100. Kobayashi T, Kao ZJL, Nakada T. Temperature dependent current–voltage and admittance spectroscopy on heat-light soaking effects of Cu(In,Ga)Se₂ solar cells with ALD-Zn(O,S) and CBD-ZnS(O,OH) buffer layers. *Solar Energy Materials and Solar Cells* 2015; **143**: 159–167. DOI:10.1016/j.solmat.2015.06.044
101. Hariskos D, Menner R, Jackson P, Paetel S, Witte W, Wischmann W, Powalla M, Bürkert L, Kolb T, Oertel M, Dimmler B, Fuchs B. New reaction kinetics for a high-rate chemical bath deposition of the Zn(S,O) buffer layer for Cu(In,Ga)Se₂-based solar cells. *Progress in Photovoltaics: Research and Applications* 2012; **20**(5): 534–542. DOI:10.1002/pip.1244
102. Löckinger J, Nishiwaki S, Fuchs P, Buecheler S, Romanyuk YE, Tiwari AN. New sulphide precursors for Zn(O,S) buffer layers in Cu(In,Ga)Se₂ solar cells for faster reaction kinetics. *Journal of Optics* 2016; **18**(8): 84002. DOI:10.1088/2040-8978/18/8/084002
103. Hildebrandt T, Loones N, Bouttemy M, Vigneron J, Etcheberry A, Lincot D, Naghavi N. Toward a better understanding of the use of additives in Zn(S,O) deposition bath for high-efficiency Cu(In,Ga)Se₂-based solar cells. *IEEE Journal of Photovoltaics* 2015; **5**(6): 1821–1826. DOI:10.1109/JPHOTOV.2015.2478066
104. Klenk R, Steigert A, Rissom T, Greiner D, Kaufmann CA, Unold T, Lux-Steiner MC. Junction formation by Zn(O,S) sputtering yields CIGSe-based cells with efficiencies exceeding 18%. *Progress in Photovoltaics: Research and Applications* 2014; **22**(2): 161–165. DOI:10.1002/pip.2445
105. Törndahl T, Hultqvist A, Platzer-Björkman C, Edoff M. Growth and characterization of ZnO-based buffer layers for CIGS solar cells. In vol 7603, 2010; 76030D–76030D–9. DOI: 10.1117/12.846351
106. Spiering S, Nowitzki A, Kessler F, Igalsen M, Abdel MH. Optimization of buffer-window layer system for CIGS thin film devices with indium sulphide buffer by in-line evaporation. *Solar Energy Materials and Solar Cells* 2016; **144**: 544–550. DOI:10.1016/j.solmat.2015.09.038
107. Kobayashi T, Jehl Li Kao Z, Kato T, Sugimoto H, Nakada T. A comparative study of Cd- and Zn-compound buffer layers on Cu(In_{1-x}Ga_x)(S_ySe_{1-y})₂ thin film solar cells. *Progress in Photovoltaics: Research and Applications* 2016; **24**(3): 389–396. DOI:10.1002/pip.2695
108. Lundberg O, Edoff M, Stolt L. The effect of Ga-grading in CIGS thin film solar cells. *Thin Solid Films* 2005; **480–481**: 520–525. DOI:10.1016/j.tsf.2004.11.080

109. Vermang B, Fjällström V, Pettersson J, Salomé P, Edoff M. Development of rear surface passivated Cu(In,Ga)Se₂ thin film solar cells with nano-sized local rear point contacts. *Solar Energy Materials and Solar Cells* 2013; **117**: 505–511. DOI:10.1016/j.solmat.2013.07.025
110. Blakers AW, Wang A, Milne AM, Zhao J, Green MA. 22.8% efficient silicon solar cell. *Applied Physics Letters* 1989; **55**(13): 1363–1365. DOI:10.1063/1.101596
111. Hsu W-W, Chen JY, Cheng T-H, Lu SC, Ho W-S, Chen Y-Y, Chien Y-J, Liu CW. Surface passivation of Cu(In,Ga)Se₂ using atomic layer deposited Al₂O₃. *Applied Physics Letters* 2012; **100**(2): 23508. DOI:10.1063/1.3675849
112. Joel J, Vermang B, Larsen J, Donzel-Gargand O, Edoff M. On the assessment of CIGS surface passivation by photoluminescence. *physica status solidi (RRL) – Rapid Research Letters* 2015; **9**(5): 288–292. DOI:10.1002/pssr.201510081
113. Kotipalli R, Vermang B, Joel J, Rajkumar R, Edoff M, Flandre D. Investigating the electronic properties of Al₂O₃/Cu(In,Ga)Se₂ interface. *AIP Advances* 2015; **5**(10): 107101. DOI:10.1063/1.4932512
114. Burgelman M, Nollet P, Degraeve S. Modelling polycrystalline semiconductor solar cells. *Thin Solid Films* 2000; **361–362**: 527–532. DOI:10.1016/S0040-6090(99)00825-1
115. Vermang B, Wätjen JT, Frisk C, Fjällström V, Rostvall F, Edoff M, Salomé P, Borme J, Nicoara N, Sadewasser S. Introduction of Si PERC rear contacting design to boost efficiency of Cu(In,Ga)Se solar cells. *IEEE Journal of Photovoltaics* 2014; **4**(6): 1644–1649. DOI:10.1109/JPHOTOV.2014.2350696
116. Vermang B, Wätjen JT, Fjällström V, Rostvall F, Edoff M, Gunnarsson R, Pilch I, Helmersson U, Kotipalli R, Henry F, Flandre D. Highly reflective rear surface passivation design for ultra-thin Cu(In,Ga)Se₂ solar cells. *Thin Solid Films* 2015; **582**: 300–303. DOI:10.1016/j.tsf.2014.10.050
117. van Lare C, Yin G, Polman A, Schmid M. Light coupling and trapping in ultrathin Cu(In,Ga)Se₂ solar cells using dielectric scattering patterns. *ACS Nano* 2015; **9**(10): 9603–9613. DOI:10.1021/acsnano.5b04091
118. Allsop N, Nürnberg R, Lux-Steiner MC, Schedel-Niedrig T. Three-dimensional simulations of a thin film heterojunction solar cell with a point contact/defect passivation structure at the heterointerface. *Applied Physics Letters* 2009; **95** (12): 122108. DOI:10.1063/1.3233962
119. Sozzi G, Pignoloni D, Menozzi R, Pianezzi F, Reinhard P, Bissig B, Buecheler S, Tiwari AN. Designing CIGS solar cells with front-side point contacts. In *Photovoltaic Specialist Conference (PVSC), 2015 IEEE 42nd*, 2015; 1–5. DOI: 10.1109/PVSC.2015.7355691
120. Bercegol A, Chacko B, Klenk R, Lauermann I, Lux-Steiner MC, Liero M. Point contacts at the copper-indium-gallium-selenide interface - a theoretical outlook. *Journal of Applied Physics* 2016; **119**(15): 155304. DOI:10.1063/1.4947267
121. Hultqvist A, Li JV, Kuciauskas D, Dippo P, Contreras MA, Levi DH, Bent SF. Reducing interface recombination for Cu(In,Ga)Se₂ by atomic layer deposited buffer layers. *Applied Physics Letters* 2015; **107**(3): 33906. DOI:10.1063/1.4927096
122. Allsop NA, Camus C, Hänsel A, Gledhill SE, Lauermann I, Lux-Steiner MC, Fischer C-H. Indium sulfide buffer/CIGS_{Se} interface engineering: Improved cell performance by the addition of zinc sulfide. *Thin Solid Films* 2007; **515**(15): 6068–6072. DOI:10.1016/j.tsf.2006.12.084
123. Fu Y, Allsop NA, Gledhill SE, Köhler T, Krüger M, Sáez-Araoz R, Blöck U, Lux-Steiner MC, Fischer C-H. ZnS nanodot film as defect passivation layer for Cu(In,Ga)(S,Se)₂ thin-film solar cells deposited by Spray-ILGAR (Ion-Layer Gas Reaction). *Advanced Energy Materials* 2011; **1**(4): 561–564. DOI:10.1002/aenm.201100146
124. Fu Y, Sáez-Araoz R, Köhler T, Krüger M, Steigert A, Lauermann I, Lux-Steiner MC, Fischer C-H. Spray-ILGAR ZnS nanodots/In₂S₃ as defect passivation/point contact bilayer buffer for Cu(In,Ga)(S,Se)₂ solar cells. *Solar Energy Materials and Solar Cells* 2013; **117**: 293–299. DOI:10.1016/j.solmat.2013.06.007
125. Koida T, Nishinaga J, Higuchi H, Kurokawa A, Iioka M, Kamikawa-Shimizu Y, Yamada A, Shibata H, Niki S. Comparison of ZnO:B and ZnO:Al layers for Cu(In,Ga)Se₂ submodules. *Thin Solid Films*. DOI: 10.1016/j.tsf.2016.03.004
126. Håla M, Fujii S, Redinger A, Inoue Y, Rey G, Thevenin M, Deprédurand V, Weiss TP, Bertram T, Siebentritt S. Highly conductive ZnO films with high near infrared transparency. *Progress in Photovoltaics: Research and Applications* 2015; **23**(11): 1630–1641. DOI:10.1002/pip.2601
127. Koida T, Fujiwara H, Kondo M. Hydrogen-doped In₂O₃ as high-mobility transparent conductive oxide. *Japanese Journal of Applied Physics* 2007; **46**(28): L685–L687. DOI:10.1143/JJAP.46.L685
128. Jäger T, Romanyuk YE, Nishiwaki S, Bissig B, Pianezzi F, Fuchs P, Gretener C, Döbeli M, Tiwari AN. Hydrogenated indium oxide window layers for high-efficiency Cu(In,Ga)Se₂ solar cells. *Journal of*

- Applied Physics* 2015; **117**(20): 205301. DOI:10.1063/1.4921445
129. Menner R, Cemernjak M, Paetel S, Wischmann W. Application of IndiumZinc Oxide window layers in Cu(In,Ga)Se₂ solar cells. In Lille (France), 2016.
 130. Sundaramoorthy R, Pern FJ, DeHart C, Gennett T, Meng FY, Contreras M, Gessert T. Stability of TCO window layers for thin-film CIGS solar cells upon damp heat exposures: part II. In vol **7412**, 2009; 74120J–74120J–12. DOI: 10.1117/12.826604
 131. Pern FJ, Noufi R, Li X, DeHart C, To B. Damp-heat induced degradation of transparent conducting oxides for thin-film solar cells. In *33rd IEEE Photovoltaic Specialists Conference, 2008. PVSC '08*, 2008; 1–6. DOI: 10.1109/PVSC.2008.4922491
 132. Guillén C, Herrero J. Stability of sputtered ITO thin films to the damp-heat test. *Surface and Coatings Technology* 2006; **201**(1–2): 309–312. DOI:10.1016/j.surfcoat.2005.11.114
 133. Feist R, Rozeveld S, Mushrush M, Haley R, Lemon B, Gerbi J, Nichols B, Nilsson R, Richardson T, Sprague S, Tesch R, Torka S, Wood C, Wu S, Yeung S, Bernius MT. Examination of lifetime-limiting failure mechanisms in CIGSS-based PV minimodules under environmental stress. In *33rd IEEE Photovoltaic Specialists Conference, 2008. PVSC '08*, 2008; 1–5. DOI: 10.1109/PVSC.2008.4922579
 134. Kempe MD, Terwilliger KM, Tarrant D. Stress induced degradation modes in CIGS mini-modules. In *33rd IEEE Photovoltaic Specialists Conference, 2008. PVSC '08*, 2008; 1–6. DOI: 10.1109/PVSC.2008.4922497
 135. Igalson M, Wimbor M, Wennerberg J. The change of the electronic properties of CIGS devices induced by the 'damp heat' treatment. *Thin Solid Films* 2002; **403–404**: 320–324. DOI:10.1016/S0040-6090(01)01510-3
 136. Kijima S, Nakada T. High-temperature degradation mechanism of Cu(In,Ga)Se₂-based thin film solar cells. *Applied Physics Express* 2008; **1**: 75002. DOI:10.1143/APEX.1.075002
 137. Lee D-W, Cho W-J, Song J-K, Kwon O-Y, Lee W-H, Park C-H, Park K-E, Lee H, Kim Y-N. Failure analysis of Cu(In,Ga)Se₂ photovoltaic modules: degradation mechanism of Cu(In,Ga)Se₂ solar cells under harsh environmental conditions. *Progress in Photovoltaics: Research and Applications* 2015; **23**(7): 829–837. DOI:10.1002/pip.2497
 138. Theelen M, Boumans T, Stegeman F, Colberts F, Illiberi A, van Berkum J, Barreau N, Vroon Z, Zeman M. Physical and chemical degradation behavior of sputtered aluminum doped zinc oxide layers for Cu(In,Ga)Se₂ solar cells. *Thin Solid Films* 2014; **550**: 530–540. DOI:10.1016/j.tsf.2013.10.149
 139. Greiner D, Gledhill SE, Köble C, Krammer J, Klenk R. Damp heat stability of Al-doped zinc oxide films on smooth and rough substrates. *Thin Solid Films* 2011; **520**(4): 1285–1290. DOI:10.1016/j.tsf.2011.04.190
 140. Hüpkens J, Owen JI, Wimmer M, Ruske F, Greiner D, Klenk R, Zastrow U, Hotovy J. Damp heat stable doped zinc oxide films. *Thin Solid Films* 2014; **555**: 48–52. DOI:10.1016/j.tsf.2013.08.011
 141. Carcia PF, McLean RS, Hegedus S. Encapsulation of Cu(In,Ga)Se₂ solar cell with Al₂O₃ thin-film moisture barrier grown by atomic layer deposition. *Solar Energy Materials and Solar Cells* 2010; **94**(12): 2375–2378. DOI:10.1016/j.solmat.2010.08.021
 142. Coyle DJ, Blaydes HA, Northey RS, Pickett JE, Nagarkar KR, Zhao R-A, Gardner JO. Life prediction for CIGS solar modules part 2: degradation kinetics, accelerated testing, and encapsulant effects. *Progress in Photovoltaics: Research and Applications* 2013; **21**(2): 173–186. DOI:10.1002/pip.1171
 143. Romanyuk YE, Hagendorfer H, Stücheli P, Fuchs P, Uhl AR, Sutter-Fella CM, Werner M, Haass S, Stükelberger J, Broussillou C, Grand P-P, Bermudez V, Tiwari AN. All solution-processed chalcogenide solar cells – from single functional layers towards a 13.8% efficient CIGS device. *Advanced Functional Materials* 2015; **25**(1): 12–27. DOI:10.1002/adfm.201402288
 144. Tsin F, Venerosy A, Vidal J, Collin S, Clatot J, Lombez L, Paire M, Borensztajn S, Broussillou C, Grand PP, Jaime S, Lincot D, Rousset J. Electrodeposition of ZnO window layer for an all-atmospheric fabrication process of chalcogenide solar cell. *Scientific Reports* 2015; **5**: 8961. DOI:10.1038/srep08961
 145. Crossay A, Buecheler S, Kranz L, Perrenoud J, Fella CM, Romanyuk YE, Tiwari AN. Spray-deposited Al-doped ZnO transparent contacts for CdTe solar cells. *Solar Energy Materials and Solar Cells* 2012; **101**: 283–288. DOI:10.1016/j.solmat.2012.02.008
 146. Vos AD. Detailed balance limit of the efficiency of tandem solar cells. *Journal of Physics D: Applied Physics* 1980; **13**(5): 839. DOI:10.1088/0022-3727/13/5/018
 147. Bremner SP, Levy MY, Honsberg CB. Analysis of tandem solar cell efficiencies under AM1.5G spectrum using a rapid flux calculation method. *Progress in Photovoltaics: Research and Applications* 2008; **16**(3): 225–233. DOI:10.1002/pip.799
 148. Wu X, Zhou J, Duda A, Keane JC, Gessert TA, Yan Y, Noufi R. High-efficiency CdTe polycrystalline thin-film solar cells with an ultra-thin CuxTe

- transparent back-contact. In *Symposium F – Thin-Film Compound Semiconductor Photovoltaics*, vol **865**, 2005; F114 (6 pages). DOI: 10.1557/PROC-865-F114
149. Kranz L, Abate A, Feurer T, Fu F, Avancini E, Löckinger J, Reinhard P, Zakeeruddin SM, Grätzel M, Buecheler S, Tiwari AN. High-efficiency polycrystalline thin film tandem solar cells. *The Journal of Physical Chemistry Letters* 2015; **6**(14): 2676–2681. DOI:10.1021/acs.jpclett.5b01108
 150. Todorov T, Gershon T, Gunawan O, Lee YS, Sturdevant C, Chang L-Y, Guha S. Monolithic perovskite-CIGS tandem solar cells via in situ band gap engineering. *Advanced Energy Materials* 2015; **5**(23). DOI:10.1002/aenm.201500799
 151. Moon SH, Park SJ, Kim SH, Lee MW, Han J, Kim JY, Kim H, Hwang YJ, Lee D-K, Min BK. Monolithic DSSC/CIGS tandem solar cell fabricated by a solution process. *Scientific Reports* 2015; **5**. DOI:10.1038/srep08970
 152. Wenger S, Seyrling S, Tiwari AN, Grätzel M. Fabrication and performance of a monolithic dye-sensitized TiO₂/Cu(In,Ga)Se₂ thin film tandem solar cell. *Applied Physics Letters* 2009; **94**(17): 173508. DOI:10.1063/1.3125432
 153. Fu F, Feurer T, Jäger T, Avancini E, Bissig B, Yoon S, Buecheler S, Tiwari AN. Low-temperature-processed efficient semi-transparent planar perovskite solar cells for bifacial and tandem applications. *Nature Communications* 2015; **6**: 8932. DOI:10.1038/ncomms9932
 154. Bailie CD, Christoforo MG, Mailoa JP, Bowring AR, Unger EL, Nguyen WH, Burschka J, Pellet N, Lee JZ, Grätzel M, Noufi R, Buonassisi T, Salles A, McGehee MD. Semi-transparent perovskite solar cells for tandems with silicon and CIGS. *Energy Environmental Science* 2015; **8**(3): 956–963. DOI:10.1039/C4EE03322A
 155. New world record for solar cell efficiency at 46% - Fraunhofer ISE. Accessed May 23, 2016. <https://www.ise.fraunhofer.de/en/press-and-media/press-releases/press-releases-2014/new-world-record-for-solar-cell-efficiency-at-46-percent>.
 156. Paire M, Shams A, Lombez L, Péré-Laperne N, Collin S, Pelouard J-L, Guillemoles J-F, Lincot D. Resistive and thermal scale effects for Cu(In, Ga)Se₂ polycrystalline thin film microcells under concentration. *Energy & Environmental Science* 2011; **4**(12): 4972. DOI:10.1039/c1ee01661j
 157. Virtuani A, Lotter E, Powalla M. Performance of Cu(In,Ga)Se-2 solar cells under low irradiance. *Thin Solid Films* 2003; **431**: 443–447. DOI:10.1016/S0040-6090(03)00184-6
 158. Powalla M, Hariskos D, Lotter E, Oertel M, Springer J, Stellbogen D, Dimmler B, Schaffler R. Large-area CIGS modules: processes and properties. *Thin Solid Films* 2003; **431**: 523–533. DOI:10.1016/S0040-6090(03)00255-4
 159. Fecher FW, Romero AP, Brabec CJ, Buerhop-Lutz C. Influence of a shunt on the electrical behavior in thin film photovoltaic modules - A 2D finite element simulation study. *Solar Energy* 2014; **105**: 494–504. DOI:10.1016/j.solener.2014.04.011
 160. Virtuani A, Lotter E, Powalla M, Rau U, Werner JH. Highly resistive Cu(In,Ga)Se-2 absorbers for improved low-irradiance performance of thin-film solar cells. *Thin Solid Films* 2004; **451**: 160–165. DOI:10.1016/j.tsf.2003.10.094
 161. Virtuani A, Lotter E, Powalla M, Rau U, Werner JH, Acciarri M. Influence of Cu content on electronic transport and shunting behavior of Cu(In,Ga)Se-2 solar cells. *Journal of Applied Physics* 2006; **99**. DOI: Artn 014906 10.1063/1.2159548
 162. Wang X, Ehrhardt M, Lorenz P, Scheit C, Ragnow S, Ni XW, Zimmer K. The influence of the laser parameter on the electrical shunt resistance of scribed Cu(In,Ga)Se-2 solar cells by nested circular laser scribing technique. *Applied Surface Science* 2014; **302**: 194–197. DOI:10.1016/j.apsusc.2013.10.155
 163. Wennerberg J, Kessler J, Stolt L. Cu(In,Ga)Se-2-based thin-film photovoltaic modules optimized for long-term performance. *Solar Energy Materials and Solar Cells* 2003; **75**: 47–55. DOI: Pii S0927-0248(02)00101-0 Doi 10.1016/S0927-0248(02)00101-0
 164. Brecl K, Topic M, Smole F. A detailed study of monolithic contacts and electrical losses in a large-area thin-film module. *Progress in Photovoltaics* 2005; **13**: 297–310. DOI:10.1002/pip.589
 165. Wehrmann A, Schulte-Huxel H, Ehrhardt M, Ruthe D, Zimmer K, Braun A, Ragnow S. Change of electrical properties of CIGS thin-film solar cells after structuring with ultrashort laser pulses. *Laser-Based Micro- and Nanopackaging and Assembly V* 2011; **7921**. Artn 79210t. DOI:10.1117/12.874999
 166. Ralph E, Woike T. Solar cell array system trades - present and future. In *37th Aerospace Sciences Meeting and Exhibit*, American Institute of Aeronautics and Astronautics, 1999.
 167. Stevens NJ. Solar array experiments on the Sphinx satellite. In 13-15 Nov. 1973, United States, 1973.
 168. Dhere NG, Ghongadi SR, Pandit MB, Jahagirdar AH, Scheiman D. CIGS2 thin-film solar cells on flexible foils for space power. *Progress in Photovoltaics: Research and Applications* 2002; **10**(6): 407–416. DOI:10.1002/pip.447

169. Tringe J, Merrill J, Reinhardt K. Developments in thin-film photovoltaics for space. In *Conference Record of the Twenty-Eighth IEEE Photovoltaic Specialists Conference, 2000*, 2000; 1242–1245. DOI: 10.1109/PVSC.2000.916114
170. Space technologies studies 2014: results. Swiss Space Office project report. February 16, 2016. Accessed May 24, 2016. http://space.epfl.ch/files/content/sites/space/files/shared/space_center/Events/MdP%202014%20Full%20Abstract%20book.pdf.
171. First Solar adding factory integrated three module systems for trackers. PV-Tech. Accessed May 8, 2016. <http://www.pv-tech.org/news/first-solar-adding-factory-integrated-three-module-systems-for-trackers>.
172. Nagy Z, Svetozarevic B, Jayathissa P, Begle M, Hofer J, Lydon G, Willmann A, Schlueter A. The adaptive solar facade: from concept to prototypes. *Frontiers of Architectural Research*. DOI: 10.1016/j.foar.2016.03.002
173. Rüggeberg M, Burgert I. Bio-inspired wooden actuators for large scale applications. *PLOS ONE* 2015; **10**(4): e0120718. DOI:10.1371/journal.pone.0120718